THERMAL DIFFUSION AND DIFFUSION IN ANISOTROPIC BINARY GAS SYSTEMS

by

ROBERT DONALD TRENGOVE, B.Sc. (Hons.)

A THESIS SUBMITTED FOR THE DEGREE OF

DOCTOR OF PHILOSOPHY

AT THE UNIVERSITY OF ADELAIDE

FEBRUARY, 1984.

DEPARTMENT OF PHYSICAL AND INORGANIC CHEMISTRY

ABSTRACT

Binary diffusion coefficients have been determined between 274 and 323 for rare gas - H_2, rare gas - D_2 and rare gas - N_2 systems.

Thermal diffusion factors were measured for He-Ar, Ar-Kr and Ne-CO_2 and for rare gas - H_2, rare gas - D_2, rare gas - N_2 and rare gas - CH_4 systems.

Both transport properties were measured in two bulb apparatus. An analysis of possible sources of error is given and where possible numerical estimations are made.

The diffusion data is used in combination with accurate second virial coefficients from the literature to derive (m68) potentials approximating the true potential of the system.

The experimental thermal diffusion factors are compared with values calculated using spherical potentials or spherical portions of anisotropic potentials. The comparison is discussed with reference to inelastic collisions and the anisotropic portion of the true potential function of the systems.

DECLARATION

I declare that this thesis contains no material accepted for any degree or diploma in any university or institution and that, to the best of my knowledge and belief, it contains no material previously published or written by any other person, except where due reference is made in the text. I give my permission for this work to be photocopied.

R.D. TRENGOVE

ACKNOWLEDGEMENTS

I have much pleasure in acknowledging the endless enthusiasm and encouragement of Dr. P.J. Dunlop under whose guidance this work was performed.

I would like to thank Mrs. H.L. Robjohns for performing the diffusion experiments for the concentration dependencies of the rare gas - hydrogen systems and for her interest in this work.

Also I would like to thank the members of the technical staff in this Department for their excellent service and co-operation.

For their constructive comments on the original draft I am grateful to Mrs. H.L. Robjohns and Dr. K.R. Harris.

I am indebted to Mrs. H.L. Robjohns and my families for their proof-reading of the manuscript; and to Mrs. L. Williams for her expertise in the typing of this thesis.

Finally, to my wife Naomi for her invaluable moral support and patience during the course of this work.

This work was completed under the tenure of a University Research Grant.

TABLE OF CONTENTS

LIST OF TABLES

LIST OF FIGURES

CHAPTER I

INTRODUCTION

Over the last two decades the accuracy of binary diffusion measurements have been improved to better than 1 percent[1,2] by van Heijningen et al,[3,4] using the two bulb technique of Ney and Armistead,[5] and Hogervorst[6] using cataphoresis. More recently this has been improved to give a precision better than 0.2 percent[7-25] using the Loschmidt[26] and two bulb techniques. This has been accompanied by similar improvements in the accuracy of the other transport properties, viscosity and thermal conductivity[2] and the quality of molecular beam experiments has been greatly enhanced by technological advances in design and construction of apparatus.

These immense improvements however have not been mirrored in thermal diffusion results because of the very small separations involved; the recent thermal diffusion results of Dunlop and coworkers[27,28] having precisions of better than 1 percent using the relationship of Laranjeira,[29] with experimental accuracy of approximately 2 percent. The results of Dunlop and coworkers using the two bulb technique agree within experimental error with the recalibrated results of Savirón et al[30] using a thermal diffusion column and reasonably well with the results of Taylor et al[31,32] using a 20-tube trennschaukel.

The very accurate transport measurements and molecular beam experiments have been used to obtain potential functions to approximate the true potential for the system with the result that

spherical potentials now exist that adequately describe the interaction for mixtures of the rare gases.

In this study diffusion coefficients and thermal diffusion factors were measured using two bulb techniques for rare gas - diatomic and rare gas - polyatomic, anisotropic systems. Details of the relevant theory and experimental procedures are outlined in Chapters III, IV and V.

The results of the measurements are given in Chapter VII as are the (m68)[33,34] potentials obtained using the diffusion coefficients. These potentials are spherical and will only approximate the 'true' potentials. Thermal diffusion factors are predicted using the expressions of Mason[35] for the potentials obtained in this study and the spherical portions of potentials from literature.

Wood and Curtiss[36] have shown that for Ar-N_2 the anisotropic portion of the potential is very important in the calculation of the thermal diffusion factor. Extending this to other systems the thermal diffusion factor is a sensitive probe of the anisotropy of the system. The comparison of experimental and calculated thermal diffusion factors in Chapter VII is viewed using the rotational relaxation studies of Kistemaker et al[37-39] and the calculations of Kelley and Wolfsberg[40] and Gelb and Kapral.[41]

Thermal diffusion factors were measured for Ne-CO_2 to investigate the anomalous results of Weissman et al[42] and the results of this study conform with the predictions of the Chapman-Enskog theory.

REFERENCES

1. T.R. Marrero and E.A. Mason, *J.Phys.Chem.Ref.Data* 1 3 (1972).
2. G.C. Maitland, M. Rigby, E.B. Smith, and W.A. Wakeham, *Intermolecular Forces*, Oxford University Press (1981).
3. R.R.J. van Heijningen, A. Feberwee, A. van Oosten and J.J.M. Beenakker, *Physica* 32 1649 (1966).
4. R.R.T. van Heijningen, J.P. Harpe and J.J.M Beenakker, *Physica* 38 1 (1968).
5. E.P. Ney and F.C. Armistead, *Phys.Rev.* 71 14 (1947).
6. W. Hogervorst, *Physica* 51 59 (1971).
7. P.J. Carson, P.J. Dunlop and T.N. Bell, *J.Chem.Phys.* 56 531 (1972).
8. M.A. Yabsley and P.J. Dunlop, *Phys.Letters* 38A 247 (1972).
9. K.R. Harris, T.N. Bell and P.J. Dunlop, *Canad.J.Chem.* 50 1874 (1972).
10. K.R. Harris, T.N. Bell and P.J. Dunlop, *Canad.J.Phys.* 50 1644 (1972).
11. P.J. Carson and P.J. Dunlop, *Chem.Phys.Lett.* 14 377 (1972).
12. P.J. Carson, M.A. Yabsley and P.J. Dunlop, *Chem.Phys.Lett.* 15 436 (1972).
13. G.R. Staker, M.A. Yabsley, J.M. Symons and P.J. Dunlop, *J.Chem.Soc., Faraday Trans.I* 70 825 (1974).
14. K.R. Harris and T.N. Bell, *Canad.J.Phys.* 51 2101 (1973).
15. G.R. Staker, P.J. Dunlop, K.R. Harris and T.N. Bell, *Chem.Phys.Lett.* 32 561 (1975).

16. M.A. Yabsley and P.J. Dunlop, *J.Phys.E:Sci.Instru.* 8 834 (1975).

17. G.R. Staker and P.J. Dunlop, *Chem.Phys.Lett.* 42 419 (1976).

18. T.N. Bell, I.R. Shankland and P.J. Dunlop, *Chem.Phys.Lett.* 45 445 (1976).

19. P.S. Arora, I.R. Shankland, M.A. Yabsley, T.N. Bell and P.J. Dunlop, *Rev.Sci.Instrum.* 48 673 (1977).

20. P.S. Arora, P.J. Carson and P.J. Dunlop, *Chem.Phys.Lett.* 54 117 (1978).

21. P.S. Arora, H.L. Robjohns, I.R. Shankland and P.J. Dunlop, *Chem.Phys.Lett.* 59 478 (1978).

22. P.S. Arora, H.L. Robjohns and P.J. Dunlop, *Physica* 95A 561 (1979).

23. P.S. Arora and P.J. Dunlop, *J.Chem.Phys.* 71 2430 (1979).

24. P.S. Arora, H.L. Robjohns, T.N. Bell and P.J. Dunlop, *Aust.J.Chem.* 33 1993 (1980).

25. H.L. Robjohns and P.J. Dunlop, *Ber. Bunsenges Phys.Chem.* 85 655 (1981).

26. J. Loschmidt, *Akad.Wiss.Wien* 61 367 (1870).

27. R.D. Trengove, H.L. Robjohns, T.N. Bell, M.L. Martin and P.J. Dunlop, *Physica* 108A 488 (1981).

28. R.D. Trengove, H.L. Robjohns, M.L. Martin and P.J. Dunlop, *Physica* 108A 502 (1981).

29. M.F. Laranjeira, *Physica* 26 409,417 (1960).

30. J.M. Savirón, C.M. Santamaria, J.A. Carrión and J.C. Yarza, *J.Chem.Phys.* 63 5318 (1975); 64 1095 (1976).

31. W.L. Taylor, S. Weissmann, W.J. Hauback and P.T. Pickett, *J.Chem.Phys.* 50 4886 (1969).

32. W.L. Taylor, *J.Chem.Phys.* 72 4973 (1980).

33. M. Klein and H.J.M. Hanley, *J.Chem.Phys.* 53 4722 (1970).

34. H.J.M. Hanley and M. Klein, *J.Phys.Chem.* 76 1743 (1972).

35. E.A. Mason, *J.Chem.Phys.* 27 75 (1957).

36. R.R. Wood and C.F. Curtiss, *J.Chem.Phys.* 70 5792,5798 (1979).

37. P.G. Kistemaker and A.E. de Vries, *Chemical Physics* 7 371 (1975).

38. P.G. Kistemaker, M.M. Hanna, A. Tom and A.E. de Vries, *Physica* 60 459 (1972).

39. P.G. Kistemaker, M.M. Hanna and A.E. de Vries, *Physica* 78 457 (1979).

40. J.D. Kelley and M. Wolfsberg, *J.Chem.Phys.* 53 2967 (1970).

41. A. Gelb and R. Kapral, *Chem.Phys.Lett.* 17 397 (1972).

42. S. Weissman, S.C. Saxena and E.A. Mason, *Phys.Fluids.* 4 643 (1961).

CHAPTER II

THE KINETIC THEORY OF GASES

2.1 *Introduction*

To give a complete and deterministic description of the state of a gas containing N molecules, one would aim to describe the positions and velocities of all the molecules as a function of time by means of classical mechanics.[1] However, even in systems whose thermodynamic state is adequately described by a virial expansion up to and including only the second virial coefficient, an extremely large number of molecules ($N \sim 10^{20}$) are present making the treatment suggested above infeasible. Therefore the problem must be analysed statistically seeking the *probable* behaviour of the entire N-molecule system.

2.2 *Chapman-Enskog Theory of Dilute Gases*

Transport properties are most readily calculated for dilute monatomic gases, the rigorous kinetic theory of which was developed independently by Chapman and Enskog.[2] In view of the complexity and length of their treatment only a brief outline of the basic assumptions and the results for binary diffusion and thermal diffusion are given here.

The Chapman-Enskog theory is centred on obtaining a solution for the single particle or first order distribution function, $f_i\ (\underset{\sim}{r},\underset{\sim}{v}_i,t)$, from the Boltzmann integro-differential equation; which describes the variation of f_i due to molecular interactions. The

function f_i, defined so that $f_i(\underset{\sim}{r},\underset{\sim}{v}_i,t)d\underset{\sim}{r},d\underset{\sim}{v}_i$ is the probable number of molecules of kind i with spatial coordinates in the range $d\underset{\sim}{r}$ about $\underset{\sim}{r}$ and velocities in the range $d\underset{\sim}{v}_i$ about $\underset{\sim}{v}_i$ at time t, describes the *probable* behaviour of any single molecule in the system.

Chapman and Enskog developed a perturbation method[3] which enabled them to solve the Boltzmann equation by expanding f_i in a series about the equilibrium distribution,

$$f_i = f_i^{(0)} + f_i^{(1)} + f_i^{(2)} \ldots . \qquad (2.1)$$

The first term, $f_i^{(0)}$ is simply the Maxwell-Boltzmann equilibrium distribution function. Truncation of the expansion (2.1) after the first correction term gives a linearised integro-differential equation for $f_i^{(1)}$ when substituted into the Boltzmann equation. The perturbation is assumed to be a linear function of the relevant transport gradient,[4,5] i.e. composition, temperature, mean velocity and pressure, and solved by further expansions in terms of the molecular velocities.[2,3] The transport coefficients can then be expressed as a ratio of two infinite determinants[2] which in general cannot be solved exactly; but a systematic truncation of the determinants allows numerical values for the coefficients to be determined. Two such approximation schemes in common usage are the method of Chapman and Cowling[2] and that of Kihara.[6] Higher approximations are obtained by taking successively larger truncated determinants.

The major assumptions inherent in the Chapman-Enskog theory

can be summarised as:-

(i) *Molecular chaos.*

This assumption is used in the derivation of the Boltzmann equation; that for two particles prior to collision, and far enough apart for molecular interactions to be ignored, there is no correlation between their velocities or position. This permits the second order distribution function to be expressed as the product of the two first order functions and hence a closed equation is produced.

(ii) *Binary Collisions.*

This assumption is also inherent in the Boltzmann equation and means that theory is limited to dilute gases where ternary and higher order collisions do not occur.

(iii) *Small molecular size.*

This allows the distribution functions f_1 and f_2 for colliding molecules 1 and 2 to be evaluated at the same point $\underset{\sim}{r}$ in space.

(iv) *Small mean free path.*

Collisions with the container walls can be neglected if the dimensions of the gas container are large in comparison to the mean free path. At very low pressures collisions with the walls predominate over intermolecular collisions and the theory is in error.

(v) *Small perturbations.*

The assumption of proportionality between the transport fluxes and gradients is only valid for small departures from equilibrium.

(vi) *Elastic collisions.*

The theory is strictly pertinent to monatomic molecules. Where molecules possess internal degrees of freedom, kinetic energy may not be conserved during collisions.

(vii) *Classical mechanics.*

The use of classical mechanics by Chapman and Enskog restricts the theory to those situations where quantum effects can be neglected. Quantum mechanical modifications of the theory[2,3] are generally unimportant except where hydrogen and helium are involved.

2.2(a) Diffusion

The Chapman-Enskog result for the diffusion coefficient, D_{12}, of a binary gas mixture to a first approximation is

$$n[D_{12}]_1 = \frac{3}{8}(kT/2\pi\mu_{12})^{\frac{1}{2}}/\sigma_{12}^2\Omega_{12}^{(1,1)^*}(T_{12}^*) \qquad (2.2)$$

In equation (2.2) n is the number density of the mixture, T is the absolute temperature and $\mu_{12} = m_1m_2/(m_1+m_2)$ the reduced molecular mass. The reduced collision integral, $\Omega_{12}^{(1,1)^*}$, is a function of the reduced temperature $T_{12}^* = kT/\epsilon_{12}$ where ϵ_{12} is the depth of the potential energy well; $\Omega_{12}^{(1,1)^*}$ is dependent upon the form of the intermolecular potential function through the dynamics of a binary

molecular encounter. The intermolecular distance at which the interaction energy is zero is denoted by σ_{12}. Both the Chapman-Cowling and the Kihara approximation schemes give the result (equation 2.2) at the first approximation.

Inspection of equation (2.2) shows that at the first approximation, the diffusion coefficient is independent of composition and inversely proportional to the number density. The composition dependence of the diffusion coefficient is born out with the introduction of the higher approximations, which may be written in the form.

$$\text{Chapman-Cowling} \quad [D_{12}]_k = [D_{12}]_1 f_D^{(k)} \tag{2.3}$$

$$\text{Kihara} \quad [D_{12}]_k = [D_{12}]_1 g_D^{(k)} \tag{2.4}$$

where k represents the degree of the approximation. The terms $f_D^{(k)}$ and $g_D^{(k)}$ represent the effect of the higher approximations.

The second approximation obtained by the Chapman-Cowling method may be written as

$$f_D^{(2)} = 1/(1-\Delta_{12}) \tag{2.5}$$

where Δ_{12} is a function of mole fractions, molecular masses, molecular sizes and reduced collision integrals. The analogous Kihara scheme expression is of the form

$$g_D^{(2)} = 1 + \Delta_{12}' \quad . \tag{2.6}$$

Explicit formula for Δ_{12} and Δ_{12}' can be found in the most relevant texts[1,2,3,6,7] and are given in Appendix I.

The experimentally-determined mutual diffusion coefficient D_{12}, which is defined in the next chapter, is related to $[D_{12}]_k$ by the following relationship

$$D_{12} = \lim_{k\to\infty} [D_{12}]_k \qquad (2.7)$$

Fortunately convergence of the approximation scheme is rapid with the third and higher approximations being almost identical. The Chapman-Cowling approximation scheme has been used in this study. This is because the Kihara scheme has only been formulated to the second approximation for thermal diffusion, whereas, the Chapman-Cowling scheme has been formulated to the third approximation.

2.2(b) Thermal Diffusion

Unlike the analogous case for diffusion (section 2.2 (a)) the Chapman-Cowling and Kihara schemes give different results for the thermal diffusion factor at the first approximation. Both however have the same general form given below.

$$[\alpha_T]_1 = (6C_{12}^* - 5)\left(\frac{x_1S_1 - x_2S_2}{x_1^2Q_1 + x_2^2Q_2 + x_1x_2Q_{12}}\right) \qquad (2.8)$$

Here x_1 and x_2 are the mole fractions and the subscripts refer to the molecular species with the usual convention that species 1 is the heavier. The term C_{12}^* is a ratio of two reduced collision integrals and the terms $S_1, S_2, Q_1, Q_2, Q_{12}$ are functions of molecular masses, molecular sizes and reduced collision integrals; expressions for these for both schemes are given in Appendix I.

The higher approximations for α_T are written in the

following form

$$\alpha_T = [\alpha_T]_1 (1 + K_{12}) \tag{2.9}$$

with the higher approximations all contained in the term K_{12}. Expressions for the higher approximations are given in the paper by Mason[6] and will not be repeated here.

2.3 *Derivation of Potential Energy Functions*

From equation (2.2), repeated here for convenience,

$$n[D_{12}]_1 = \frac{3}{8} (kT/2\pi\mu_{12})^{\frac{1}{2}}/\sigma_{12}^2 \; \Omega_{12}^{(1,1)^*} \; (T_{12}^*) \tag{2.10}$$

it is apparent that a knowledge of the intermolecular potential function permits calculation of the diffusion coefficient or *vice versa*, measurements of the diffusion coefficient may yield information concerning the potential function.

Equation (2.10) can be written in terms of the pressure, P, to give

$$P[D_{12}]_1 = \frac{3}{8\sigma_{12}^2} \left(\frac{k^3}{2\pi\mu_{12}}\right)^{\frac{1}{2}} \frac{T^{3/2}}{\Omega_{12}(1,1)^*} \tag{2.11}$$

or $$Y_i = \phi X_i \tag{2.12}$$

where $$\phi = \frac{3}{8\sigma_{12}^2} \left(\frac{k^3}{2\pi\mu_{12}}\right)^{\frac{1}{2}} . \tag{2.13}$$

Smoothed values of D_{12} extrapolated to $x_1 = 0$, using the experimentally determined concentration dependence, and corrected to the theoretical *first* approximation, using the Chapman-Enskog theory for the concentration dependence of D_{12}[8], can be used in

equation (2.12) for an assumed potential form and approximate value for ε_{12}. The best value of ε_{12} may then be determined by least-squaring the (Y_i, X_i) values to pass through the origin for a series of ε_{12} values and selecting the value with the minimum standard error. A value of σ_{12} is obtained from the best value of the slope, ϕ.

This procedure is fine tuned using second virial coefficients[9] to differentiate between pairs of potential parameters.

Reduced collision integrals and the corresponding reduced second virial coefficients have been tabulated[10] for the (m,6,8) potentials.

The diffusion coefficient measured over a range of temperatures fixes the position and the slope of the repulsive wall of the potential energy function.[11]

The second virial coefficient, B_{12}, however, if available over a large temperature range gives information about the location of the wall and the volume of the attractive well of the potential energy function.

Consequently potential energy functions derived using the preceding discussion will not describe the long range part of the 'true' potential energy function correctly.

REFERENCES

1. G.C. Maitland, M. Rigby, E.B. Smith, and W.A. Wakeham, *Intermolecular Forces*, Oxford University Press (1981).
2. S. Chapman and T.G. Cowling, *The Mathematical Theory of Non-uniform Gases*, 3rd edition, Cambridge University Press (1970).
3. J.O. Hirschfelder, C.F. Curtiss and R.B. Bird, *Molecular Theory of Gases and Liquids*, Wiley, New York (1954).
4. E.A. Mason, R.J. Munn and F.J. Smith, *Advances in Atomic and Molecular Physics*, p. 33, Volume 2, Academic Press, New York (1966).
5. K.E. Grew, *Transport Phenomena in Fluids*, Chapter 10, Ed. H.J.M. Hanley, Dekker, New York. (1969).
6. E.A. Mason, *J.Chem.Phys.* 27 75,782 (1957).
7. T.R. Marrero and E.A. Mason, *J.Phys.Chem. Ref. Data* 1 3 (1972).
8. K.R. Harris, T.N. Bell and P.J. Dunlop, *Canad.J.Phys.* 50 1644 (1972).
9. P.S. Arora, P.J. Carson and P.J. Dunlop, *Chem.Phys.Letters* 54 117 (1978).
10. M. Klein, H.J.M. Hanley, F.J. Smith and P. Holland, *Tables of Collision Integrals and Second Virial Coefficients for the (m,6,8,) Intermolecular Potential Functions*, US National Bureau of Standards Circular, NSRD-NBS47 (1974).
11. R.T. Pack, *Private communication.*

CHAPTER III

BASIS OF EXPERIMENTAL METHODS

3.1 *Introduction*

Diffusion may be defined as that process whereby a *relative flow* of components is caused by the presence of a potential gradient. Although most frequently associated with a non-uniformity in composition, diffusion can also arise as a result of a non-uniformity in pressure or temperature or from the influence of some external force. The diffusion types of interest here are those arising from a non-uniformity in

i) concentration, termed *ordinary diffusion* and

ii) temperature, termed *thermal diffusion*.

In the absence of any external forces, a system, in which isothermal and isobaric conditions prevail, will only exhibit diffusion if there is a concentration gradient. Here the direction of matter flow is such that the components of the system become uniformly distributed and the process is termed isothermal diffusion. However, it must be noted that the transport of matter produces a flow of energy and consequently temperature gradients; this phenomenon is known as the Dufour[1] effect or diffusion thermo effect and its consequences will be neglected for the moment. In addition, transport of matter produces a pressure gradient; however, this is negligible except in the case of diffusion along a capillary.[2]

If in the same system the concentration and pressure are uniform but a temperature gradient develops, a concentration gradient

will also develop and this increases until the separating effect of thermal diffusion is balanced by the mixing effect of ordinary diffusion. Thus, in the steady state where there is non-uniformity of temperature, there is non-uniformity of composition.

The Dufour effect and thermal diffusion are converse phenomena and, being second order in nature, neither can be satisfactorily explained by elementary kinetic theory; however both phenomena are predicted by the rigorous Chapman-Enskog theory.

For the remainder of this report, ordinary diffusion will simply be referred to as diffusion.

3.2 *Diffusion-Flow Equations and Frames of Reference*

Although diffusion is generally a three-dimensional process the present discussion is simplified by considering the flow of matter in a single dimension. What follows is strictly pertinent to those systems where isothermal conditions exist.

Most discussions of diffusion begin with the statement first formulated by Fick[3] in 1855 which is now known as Fick's first law of diffusion; the rate of mass transfer is proportional to the relevant concentration gradient. To make use of this law it is necessary to specify the *frame of reference* to which the measurements apply and to show that Fick's law is applicable in this frame. Experimental observations are generally based on a reference frame defined by the diffusion cell[4] whereas the phenomenological flow equations[5,6] are discussed in terms of more general reference frames. In experimental situations the *volume-fixed* frame, defined as that reference frame

moving with the same velocity as the *local* centre of volume, is of importance.[6,7] Thus the conditions under which the flux in the different reference frames can be equated must be defined.

For a binary system the relationship between the fluxes, J_i, in the volume-fixed frame is

$$\sum_{i=1}^{2} \bar{V}_i (J_i)_V = 0 \qquad (3.1)$$

where J_i is the local flux of component i, defined as the number of moles of i crossing unit area normal to the direction of diffusion in unit time, and $\bar{V}_i$ is the partial molar volume of species i. The subscripts V on (J_i) implies that each flux is measured with respect to the volume frame of reference.

In this frame Fick's first law may be expressed mathematically as

$$(J_i)_V = -(D_i)_V (\partial C_i/\partial z)_t \quad (i = 1,2) \qquad (3.2)$$

where C_i is the concentration of component i (moles/unit volume), the proportionality constant, $(D_i)_V$, is the diffusion coefficient and z specifies the direction of diffusion. Combining equations (3.1) and (3.2) with the thermodynamic relation

$$\sum_{i=1}^{2} C_i \bar{V}_i = 1 \qquad (3.3)$$

it is possible to show that

$$(D_1)_V = (D_2)_V = (D_{12})_V \qquad (3.4)$$

where $(D_{12})_V$ is the mutual diffusion coefficient.

But, as mentioned earlier, most experimental observations are based on the reference frame defined by the cell;[4] and diffusion in *real* fluids is often complicated by volume changes which cause the system to experience a bulk flow.

Therefore, the volume-fixed reference frame cannot be considered stationary[8] with respect to the cell frame. If U_{VC} denotes the relative velocity of the two frames and $(J_i)_C$ is the flux of component i in the cell frame, then the relationship between the two fluxes[5] is

$$(J_i)_C = (J_i)_V + C_i U_{VC} \qquad (i = 1,2) \quad . \qquad (3.5)$$

Kirkwood et al[5] have shown that the conditions under which the second term in equation (3.5) vanishes is that (for component 1)

$$(\partial \overline{V}_1 / \partial C_1) = 0 \qquad (3.6)$$

This condition is always obeyed by *real gaseous systems* in the low density limit.[9]

Thus equation (3.2) may be written as

$$(J_i)_C = -(D_{12})_V (\partial C_i / \partial z)_t \qquad (i = 1,2) \quad . \qquad (3.7)$$

On combining equation (3.7) with the pertinent equations of continuity[6] for a chemically inert system, which may be expressed as

$$(\partial (J_i)_C / \partial z)_t = -(\partial C_i / \partial t)_z \qquad (i = 1,2) \qquad (3.8)$$

a mathematical statement of Fick's second law of diffusion results

$$(\partial C_i / \partial t)_z = \left[\frac{\partial}{\partial z} \left(D_{12} \frac{\partial C_i}{\partial z} \right) \right]_t \qquad (i = 1,2) \quad . \qquad (3.9)$$

Here the subscript V has been omitted for simplicity. Equation (3.9) is generally written in the form

$$(\partial C_i/\partial t)_z = D_{12}(\partial^2 C_i/\partial z^2)_t \quad (i = 1,2) \qquad (3.10)$$

when the diffusion coefficient is independent of concentration.

In actual fact D_{12} is slightly concentration dependent, but Ljunggren[10] has shown that to a first approximation the measured diffusion coefficient corresponds to the mean concentration at the end of the experiment.

3.3 *Diffusion - Two Bulb Technique*

The two bulb method for studying diffusion was developed by Ney and Armistead[11] in order to determine the self-diffusion coefficient of UF_6. The apparatus consists of two bulbs or chambers connected by a narrow tube through which diffusion occurs. After an initial transient, the composition of the bulbs varies exponentially with time and D_{12} can be found from the relaxation time.

A detailed analysis of the two bulb cell is found in the paper by Ney and Armistead, so only the assumptions and results will be given here.

Ney and Armistead made the following assumptions:

(i) A quasi-stationary state exists implying that the flux of a component is constant along the connecting tube, and, therefore a linear variation in composition exists.

(ii) The concentration gradient is entirely contained in the connecting tube.

(iii) The volume of the connecting tube is negligible compared with the volume of the bulbs.

If C_{1U} is the concentration of component 1, the heavy component, in the upper bulb of volume V_U and C_{1L} is the concentration in the lower bulb of volume V_L then at time t the difference in concentration between the bulbs is given by

$$C_{1U}(t) - C_{1L}(t) = (C_{1U}(0) - C_{1L}(0)) \exp(-t/\tau) \quad (3.11)$$

where $$\tau = \frac{1}{D_{12}}\left(\frac{L}{A}\right)\left(\frac{1}{V_U} + \frac{1}{V_L}\right) \quad . \quad (3.12)$$

The terms $C_{1U}(0)$ and $C_{1L}(0)$ are the initial concentrations in the bulbs and τ is the so called "relaxation time". Equations (3.11) and (3.12) indicate that measurements as a function of time of the composition difference between the two bulbs will give the relaxation time, allowing the calculation of D_{12} from cell dimensions. Equations (3.11) and (3.12) are only valid when the apparatus conforms to the assumptions of Ney and Armistead, and in reality all of the assumptions may be invalid or unnecessary.[12]

The assumption of a quasi-stationary state is only valid in the limit of a narrow connecting tube joining two infinitely large bulbs. Annis et al[13] have developed a corrected expression for the relaxation time assuming only that the mean flux in the tube is proportional to the effective mean flux at the two ends of the tube. The corrected expression for the relaxation time is

$$\tau = \frac{K}{D_{12}}\left(\frac{L}{A}\right)\left(\frac{1}{V_U} + \frac{1}{V_L}\right) \quad (3.13)$$

where K contains the correction to deviation from a quasi-stationary state and is a function of the bulb volumes.[12] Thus the apparatus design should be such that the deviation of K from unity is minimised,

also aiding the conformity of the apparatus to the third assumption of Ney and Armistead.

The second assumption of Ney and Armistead requires an end correction as the gradient extends into the bulbs, resulting in an effective length, L_{eff}, greater than the dimension of the connecting tube,

$$L_{eff} = L + 2\alpha R \quad . \quad (3.14)$$

Here R is the radius of the tube and α is a numerical constant dependent on the end geometry of the tube. Wirz[14] investigated the problem of end correction variation for tubes differing in annulus width, diameter and length. Yabsley and Dunlop[15] have treated Wirz's results statistically giving excellent agreement with the generally acceptable values of α from the analogous case of sound passage in a tube.[16,17]

Yabsley and Dunlop[15] and Arora et al[18] have measured diffusion coefficients in a two bulb cell using different connecting tubes and found that the Wirz relation[14,15] did not satisfactorily correlate the data obtained with the different tubes. They concluded that either the method used to apply the end correction is incomplete or there is another unknown factor involved.[18] In the same laboratory diffusion coefficients have been measured using the Loschmidt technique[19] with an accuracy of better than 0.2%.[20-23] The results from both methods have been compared and the 'two-bulb' results differ from those of the 'Loschmidt' technique by approximately 0.5%. The results of the Loschmidt cell were used to calibrate the two-bulb cell at 300K, making a knowledge of the cell dimensions

unnecessary. The calibration at 300K has been shown to be valid over ±25K using O_2-Ar.[24,25]

3.4 *Thermal Diffusion - Introduction*

Several attempts have been made to give a simple explanation of thermal diffusion in gases similar to the elementary treatment of the other transport phenomena. Fürth[26] used an extension of the mean-free-path argument of elementary discussions of viscosity and ordinary diffusion. In this treatment he made a distinction between the mean-free-path for transport of number and the mean-free-path for transport of mean thermal speed, leading to an expression for the thermal diffusion factor of the same form as that obtained by the rigorous theory; thus some qualitative information can be deduced from it. Laranjeira[27,28] developed Fürth's treatment and extended it to multicomponent mixtures and in doing so found that the inverse of the thermal diffusion factor is a linear function of the concentration. This relationship has been checked experimentally on a number of systems[28-32] and found to hold within experimental error.

3.5 *Thermal Diffusion - Flow equations*

If the local flux of component i in a binary system is denoted by J_i and defined as the number of molecules of i crossing unit area normal to the direction of diffusion is unit time. Then the relationship between the fluxes in the reference frame that moves with the molecular number-average velocity is, for a binary system

$$\sum_{i=1}^{2} J_i = 0 \qquad (3.15)$$

(This is analogous to equation (3.1) where $(J_i)_V = J_i/\overline{V}$).

In this reference frame the phenomenological flux equations for the two components can be written as follows:

$$J_1 = -nD_{12}\nabla x_1 - nD_T\nabla \ln T + nD_p\nabla \ln p \qquad (3.16)$$

$$J_2 = -nD_{21}\nabla x_2 + nD_T\nabla \ln T - nD_p\nabla \ln p \qquad (3.17)$$

where J_1 and J_2 are the flux densities, defined above, n is the total number density, x_1 and x_2 are mole fractions, D_{12} and D_{21} are ordinary diffusion coefficients, D_T is the coefficient of thermal diffusion and D_p is the coefficient of pressure diffusion. Diffusion due to external forces is neglected in these equations.

It has been shown previously that $D_{12} = D_{21}$; equation (3.4), and the pressure diffusion terms in equations (3.16) and (3.17) are only relevant for diffusion along a capillary[2] and may be neglected here.

The sign reversal of the thermal diffusion term between the two flux equations necessitates that some sign convention be adopted; the convention is;

(i) component 1 is the heavy component

(ii) if component 1 concentrates in the cold region, then D_T is positive.

Because the coefficient D_T has a very strong dependence on composition equations (3.16) and (3.17) are usually written in terms

of the *thermal diffusion factor* α_T, defined by the relation

$$\alpha_T = \frac{1}{x_1 x_2} \cdot \frac{D_T}{D_{12}} \quad . \qquad (3.18)$$

Thus equation (3.16) may be written as

$$J_1 = -nD_{12}(\nabla x_1 + x_1 x_2 \alpha_T \nabla \ln T) \quad . \qquad (3.19)$$

3.6 *Thermal Diffusion - The two-bulb technique*

Of the various methods that have been used to study gaseous thermal diffusion, the two bulb technique is the simplest and the most accurate[33] provided that the separations involved are reasonably large.

The technique entails maintaining two bulbs, that are connected by a small tube, at different uniform temperatures. The temperature gradient occurs entirely along the connecting tube and the apparatus is mounted vertically to avoid convection. The temperature gradient is maintained until the system has achieved a steady state, at which point the net flux in the system is zero, and equation (3.19) becomes

$$-nD_{12}(\nabla x_1 + x_1 x_2 \alpha_T \nabla \ln T) = 0 \qquad (3.20)$$

or

$$\nabla x_1 = -x_1 x_2 \alpha_T \nabla \ln T \quad . \qquad (3.21)$$

In the following discussion a prime on a variable indicates that it corresponds to the higher temperature.

If the temperatures at which the bulbs are maintained are T and T′, and x_1 and x_2 are the mole fractions of the species in the bulb maintained at temperature T and x_1' and x_2' are the mole fractions

of the species in the bulb maintained at temperature T', then equation (3.21) is integrated from $T \rightarrow T'$ and $x_1 \rightarrow x_1'$ and we obtain

$$\ln((x_1/x_2)/(x_1'/x_2')) = \alpha_T \ln(T'/T) \quad . \quad (3.22)$$

This is generally written as

$$\ln((x_1/(1-x_1))/(x_1'/(1-x_1'))) = \alpha_T \ln(T'/T) \quad (3.23)$$

and α_T is assumed to be a constant over the relevant range of temperature and composition. The term $(x_1/(1-x_1))/(x_1'/(1-x_1'))$ is usually referred to as the separation factor, q.

The ratio $\ln q/\ln(T'/T)$ gives an experimental mean value of the thermal diffusion factor α_T over the range $T \rightarrow T'$; thus it is necessary to assign a temperature to the value of α_T thus obtained. This temperature assignment depends on the variation of α_T over the range from T to T'. Several simple formulas[31,34-36] have been used to approximate the temperature dependence of α_T, with the formula of Brown[34] being most widely used.

Brown found that α_T varied with temperature as follows

$$\alpha_T = a - b/T \quad (3.24)$$

giving a mean temperature, $\bar{T}$, to which the α_T value obtained from equation (3.23) may be assigned as

$$\bar{T} = \frac{T'T}{T'-T} \ln\left(\frac{T'}{T}\right) \quad . \quad (3.25)$$

Paul et al[31] found that α_T varied linearly with temperature

$$\alpha_T = a + bT \quad (3.26)$$

and

$$\bar{T} = (T'-T)/\ln\left(\frac{T'}{T}\right) \quad . \quad (3.27)$$

In equations (3.24) and (3.26) a and b are constants.

For this work the $\overline{T}$ to which experimentally determined values of α_T were assigned was that described by equation (3.27) as, shown in Chapters 6, 7, both theory and experiment show the thermal diffusion factor to be a linear function of temperature.

3.7 *Thermal Diffusion - Approach to steady-state*

The approach to the steady-state was first investigated by Blüh et al[37] in 1937 and their results indicated an approximately exponential rate of approach.

Jones and Furry[38] developed an approximate theory to describe the approach to the steady-state, which gives an exponential rate of approach,[35] with the following expression for the relaxation time.

$$\tau = 1/b = \frac{NN'}{N+N'} \frac{L}{nD_{12}A} \frac{T}{\Delta T} \ln(T'/T) \quad . \quad (3.28)$$

Here L is the length of the connecting tube, A is the cross-sectional area, N and N' are the number of molecules in the bulbs maintained at the temperatures T and T' respectively, n is the number density of both species and D_{12} the diffusion coefficient.

The important features of equation (3.28) are that the relaxation time τ is

(i) proportional to the length of the connecting tube,

(ii) inversely proportional to the cross-section of the connecting tube

(iii) inversely proportional to some mean diffusion coefficient D_{12},

(iv) varies directly with pressure through the diffusion coefficient, as nD_{12} is a constant.

In 1954 Nettley[40] confirmed experimentally the exponential rate of approach to the steady state and subsequent experimental confirmations have been performed by van Itterbeek and Nihoul[39] and by Lonsdale and Mason.[36]

REFERENCES

1. L. Dufour, *Pogg.Ann.* 148 490 (1873).
2. K.P. McCarty and E.A. Mason, *Phys.Fluids* 3 908 (1960).
3. A. Fick, *Ann.Phys.Chem.* 94 59 (1855).
4. P.J. Dunlop, B.J. Steel and J.E. Lane in *Physical Methods of Chemistry*, Vol. 1, edited by A. Weissberger and B. Rossiter, Wiley (1972).
5. J.G. Kirkwood, R.L. Baldwin, P.J. Dunlop, L.J. Gosting and G. Kegeles, *J.Chem.Phys.* 33 1505 (1960).
6. D.D. Fitts, *Non-equilibrium thermodynamics*, McGraw-Hill (1962).
7. G.S. Hartley and J. Crank, *Trans.Faraday Soc.* 45 801 (1949).
8. L. Onsager, *Ann.N.Y.Acad.Sci.* 46 241 (1945).
9. I.R. Shankland, *Ph.D. Thesis*, University of Adelaide (1979).
10. S. Ljunggren, *Ark.Kemi* 24 1 (1965).
11. E.P. Ney and F.C. Armistead, *Physical Review* 71 14 (1947).
12. T.R. Marrero and E.A. Mason, *J.Phys.Chem.Ref.Data* 1 3 (1972).
13. B.K. Annis, A.E. Humphreys and E.A. Mason, *Phys.Fluids* 12 78 (1969).
14. P. Wirz, *Helv.Phys.Acta* 20 3 (1947).
15. M.A. Yabsley and P.J. Dunlop, *Physica* 85A 160 (1976).
16. Lord Rayleigh, *The Theory of Sound II*, p. 203, 491. Dover Publications, New York (1945).
17. L.V. King, *Phil.Mag.* 21 128 (1936).
18. P.S. Arora, I.R. Shankland, T.N. Bell, M.A. Yabsley and P.J. Dunlop, *Rev.Sci.Instrum.* 48 673 (1977).

19. J. Loschmidt, *Akad.Wiss.Wien.* 61 367 (1870).

20. G.R. Staker and P.J. Dunlop, *Rev.Sci.Instrum.* 47 1190 (1976).

21. I.R. Shankland and P.J. Dunlop, *Chem.Phys.Lett.* 39 557 (1976).

22. G.R. Staker and P.J. Dunlop, *Chem.Phys.Lett.* 42 419 (1976).

23. T.N. Bell, I.R. Shankland and P.J. Dunlop, *Chem.Phys.Lett.* 45 445 (1977).

24. P.S. Arora, H.L. Robjohns, T.N. Bell and P.J. Dunlop, *Aust.J.Chem.* 33 1993 (1980).

25. P.J. Dunlop, *Private communication.*

26. R. Fürth, *Proc.Roy.Soc. (London)* A179 461 (1942).

27. M.F. Laranjeira, *Physica* 26 409 (1960).

28. M.F. Laranjeira, *Physica* 26 417 (1960).

29. M.F. Laranjeira and J. Kistemaker, *Physica* 26 431 (1960).

30. E.A. Mason, S. Weissman and R.P. Wendt, *Phys.Fluids* 7 1011 (1964).

31. R. Paul, A.J. Howard and W.W. Watson, *J.Chem.Phys.* 43 1622 (1965).

32. R.D. Trengove, H.L. Robjohns, T.N. Bell, M.L. Martin and P.J. Dunlop, *Physica* 108A 488 (1981).

33. E.A. Mason, R.J. Munn and F.J. Smith, *Advances in Atomic and Molecular Physics*, Vol. 2, Academic Press, New York (1966).

34. H. Brown, *Phys.Rev.* 58 661 (1940).

35. K.E. Grew and H.L. Ibbs, *Thermal Diffusion in Gases*, Cambridge University Press, London (1952).

36. H.K. Lonsdale and E.A. Mason, *J.Phys.Chem.* 61 1544 (1957).

37. G. Blüh, O. Blüh and M. Puschner, *Phil.Mag.* 24 1103 (1937).

38. R.C. Jones and W.H. Furry, *Rev.Mod.Phys.* 18 151 (1946).

39. A. van Itterbeek and J. Nihoul, *Acustica* 5 142 (1955).

40. P.T. Nettley, *Proc.Phys.Soc.(London)* B67 753 (1954).

CHAPTER IV

EXPERIMENTAL APPARATUS AND PROCEDURE

4.1 *Diffusion Cell Description*

A diagram showing the important features of the diffusion cell is given in Figure 4.1. It is similar in design to a cell used previously,[1] but was machined from one block of stainless steel and designed so that precision bore connecting tubes of different dimensions could be inserted.

The connecting tubes, or inserts, were fabricated from brass and copper and were made with an external taper along the length of 0.002 cm. The minimum external diameter of the insert was exactly the same size as the internal diameter of the section of the stainless steel block to house it, which had been honed out so that it was constant to better than 0.001 cm. The inserts were press fitted into position.

The two bulbs were formed by bolting stainless steel end plates to the block with lead o-rings placed in circular V-shaped grooves as vacuum seals. The grooves were designed to eliminate any free space between the metal-metal surface. The cell was vented by Nupro bellows valves that had been argon welded into the end plates.

The concentration changes in the bulbs during experiments were monitored with thermistors (Fenwal type G112P) and viton o-rings formed vacuum seals between the cell and thermistors.

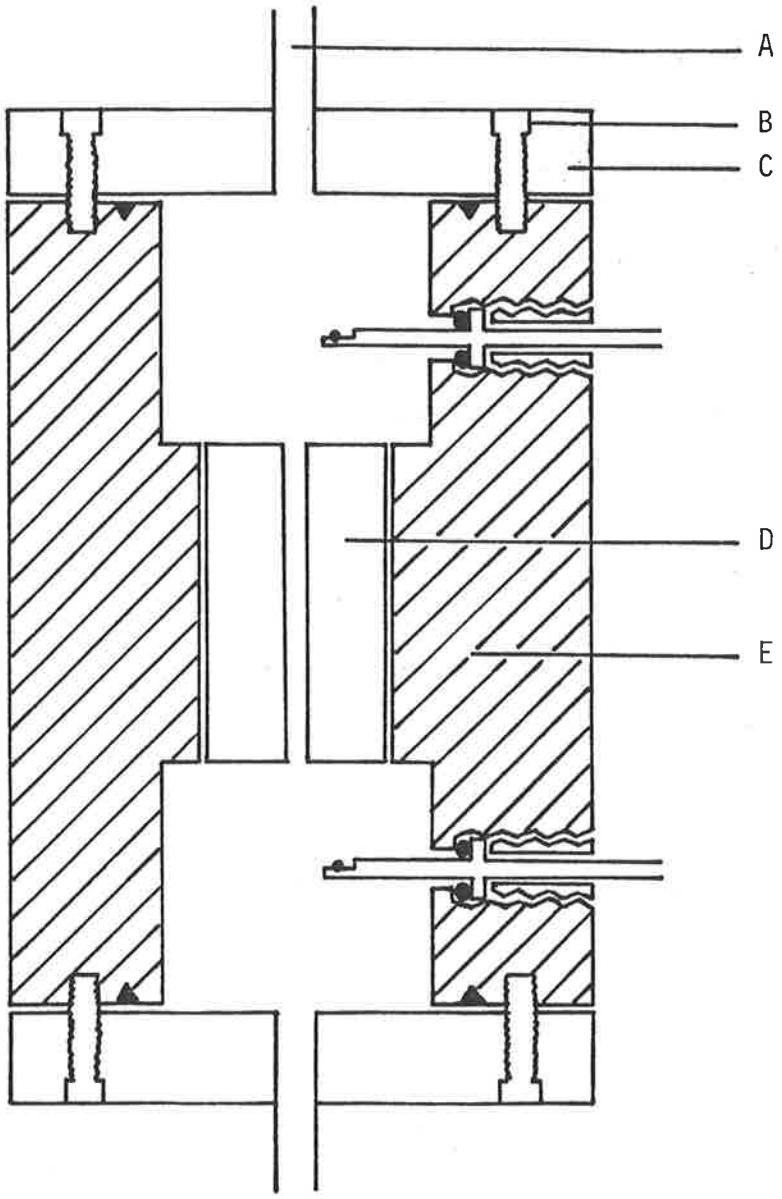

Figure 4.1. Two Bulb Diffusion Cell

A - inlet; B - bolts; C - cell end; D - insert;

E - cell body; ● - silicone rubber o-rings;

▲ - lead o-rings.

Electrical connections with the Wheatstone bridge were made with shielded two-core cable. Details of the thermistors and bridge circuit are given in Chapter V.

The cell dimensions are given in table 4.1.

The two inserts described in table 4.1 were sufficient to give convenient relaxation times for the systems studied.

The cell was suspended vertically in a water bath containing 500 litres of water. The valves on the cell ends were connected to the external apparatus, comprising gas cylinders, vacuum system and pressure gauge, by a manifold constructed of stainless steel tubing.

The leak rate in the cell and manifold was better than 2×10^{-6} Torr/min.

Table 4.1

Dimensions of the Diffusion Cell

Block			
Length		10.65	cm
Outer Diameter		7.60	cm
Inner Diameter (bulbs)		3.50	cm
Inner Diameter (insert)		2.54	cm
Bulb depth		3.20	cm
Insert depth		4.25	cm
End Plates			
Diameter		7.60	cm
Thickness		1.25	cm
Inserts			
I1	Length	4.25	cm
	Internal Diameter	0.16	cm
I2	Length	4.25	cm
	Internal Diameter	0.25	cm

4.2 *Experimental Procedure for Diffusion*

All experiments were performed in the following way.

The first gas was introduced into the cell and the cell contents isolated after attaining thermal equilibrium. A second gas was then introduced in to the manifold of the apparatus at a greater pressure than that within the cell and allowed to attain thermal equilibrium. This second gas was then admitted into the appropriate bulb, depending upon the relative densities of the gases, so that gravitational stability was maintained during diffusion. For experiments in the intermediate mole fraction range the above procedure was used to make up mixtures to which a further amount of the second gas was admitted to attain the desired mole fraction. The latter procedure reduced the deviation of the system from equilibrium.

Pressure measurements were made using a Texas Instruments Bourdon-tube gauge. The Bourdon-tube consisted of a quartz spiral and was intended for use over the pressure range from 0 to 101 kPa. The pressure gauge was calibrated against a dead weight tester (Bell and Howell, type 6-201-0001 primary pressure standard) in this laboratory. The calibration was reproducible to within 0.03% and corrected to account for the difference between local gravitational acceleration[2] (9.79724 ms^{-2}) and the standard value (9.80665 ms^{-2}); the accuracy of the dead weight tester was stated as better than 0.025%.

Throughout all experiments, the temperature of the thermostatted bath was controlled to within ±0.002K by means of a thermistor bridge

temperature controller containing an instrument operational amplifier, Type 725, adjusted for a gain of 300 000. A refrigeration unit with a by-pass valve was used to cool water in a second bath, and this water was pumped through a heat-exchanger to control the temperature of the diffusion thermostat for temperatures below 300K. Mercury-in-glass thermometers, which had been calibrated against a platinum resistance thermometer, were used to monitor the bath temperature.

The thermistors were used to monitor the change in composition in the bulbs with time; measurements being taken at fixed time intervals. The procedure for obtaining diffusion coefficients from these measurements is given in Chapter V.

4.3 *Thermal Diffusion Cell Description*

A diagram showing the important features of the cell is shown in Figure 4.2. The cell has been used previously in this laboratory[3,4] and consists basically of two bulbs joined by a length of tubing.

In previous work[3,4] cylindrical brass bulbs were used, and the lead o-ring seals between the brass and stainless steel endplates were susceptible to corrosion at the temperatures used. To avoid this problem steel cylindrical bulbs with argon welded end plates and taps (Nupro bellows valves), were used.

The cell is 94 cm in length and the bulbs are attached to the main frame of the unit by means of pairs of FC38 vacuum flanges. The bulbs had an internal diameter of 11.5 cm and an external diameter of

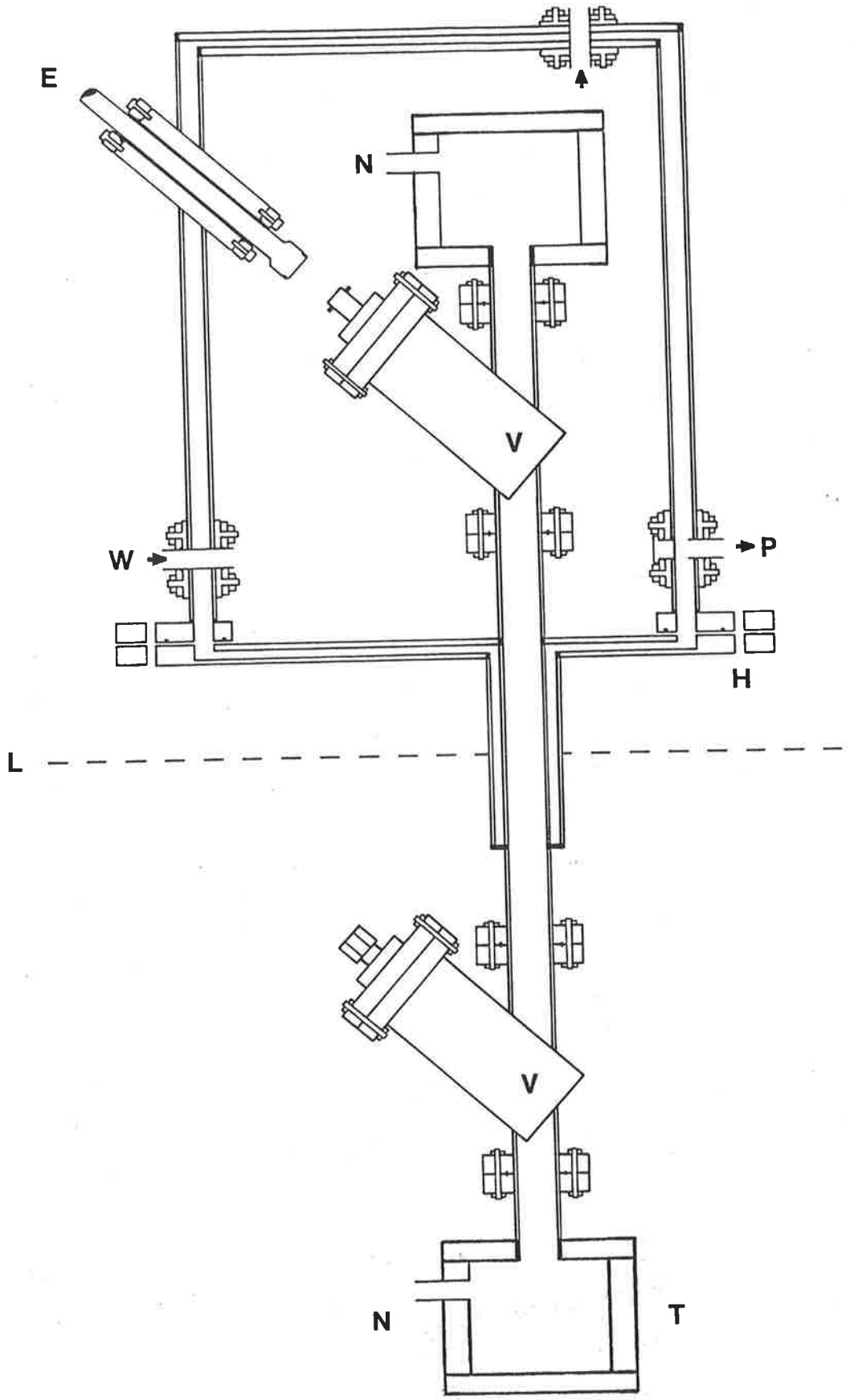

Figure 4.2 Thermal Diffusion Cell and Canopy

14.0 cm and are 12.5 cm in length. Two stainless steel bellows valves, V (Vacuum Generators, England), allow the gas mixture in the bulbs to be isolated from the gas in the separating tube, S, when required. The bellows valves are connected to the separating tube by means of pairs of FC38 vacuum flanges.

The taps on the bulbs allowed the cell to be connected to the analysis apparatus (see Chapter V) for filling to begin an experiment and for analysis of the bulb contents at the end of an experiment.

4.4 *Thermal Diffusion Procedure.*

To begin an experiment the cell, previously evacuated with a leak rate better than 0.2×10^{-5} Torr/min, was filled with a previously prepared gas mixture, one of the calibration mixtures (see section 5.5). For all experiments the cell was filled to a pressure of 33 kPa.

Pressure measurements were made using a 100 mbar Schlumberger pressure transducer with a digital readout. The pressure transducer was calibrated with a Texas Instruments Bourdon-tube gauge and this calibration had a reproducibility of within 0.1%.

Using a small 'boat winch' and a pulley attached to the ceiling the cell was then manoeuvred into a vertical position with the cell inverted. The canopy, C, was at this stage attached to the main cell frame with bolts passing through the holes, H, and the cell swung into the upright position indicated in Figure 4.2. Two silicone o-rings provided water and vacuum seals between the canopy

and the cell frame. With the canopy bolted in position its vacuum jacket interconnected with the concentric jacket on the connecting tube, thus ensuring a reproducible temperature gradient between the two bulbs for the duration of the experiment.

The cell unit was then lowered into a thermostatted bath of capacity 300 l., so that the bottom bulb and valve were immersed to the level L shown in Figure 4.2. Then water from a second thermostatted bath at a higher temperature was pumped through the canopy at 30 l/min entering at port W1 and leaving at port W2. The jacket encasing the canopy and the connecting tube was then evacuated to 10^{-5} Torr using an oil diffusion pump.

After achievement of a steady state the valves were closed simultaneously, isolating the gas samples in the bulbs.

Temperatures in both baths were monitored with a platinum resistance thermometer (Leeds and Northrup) in conjunction with a Smith No.3 resistance bridge (Croydon Precision Instrument Co.).

The cell unit was then removed from the bath and the canopy removed from the top of the cell and one of the bulb taps connected to the analysis apparatus. The contents of the two bulbs were analysed after being left overnight to equilibrate to ambient temperature.

Both of the baths used were equipped with refrigeration units with a bypass valve and these were used when temperatures below room temperature were required. A water-alcohol mixture was used in the cold bath when temperatures below 273K were required.

4.5 *Relaxation time of the thermal diffusion cell.*

The volume of the stainless steel bulbs used in this study is approximately twice that of the brass bulbs used previously.[3] The result of Jones and Furry,[5,6] given in equation (3.28) and repeated here for convenience.

$$\tau \cong \frac{NN'}{N+N'} \frac{L}{nD_{12}A} \frac{T}{\Delta T} \ln (T'/T) \qquad (4.1)$$

indicates that for a given system the relaxation time using the new bulbs should be approximately twice that using the brass bulbs if the pressure in the cell is unchanged. However, equation (4.1) further indicates that the relaxation time, τ, is directly proportional to the pressure; thus if the pressure for this study is half that used previously the relaxation time will be essentially unchanged. The system Xe-N_2 was used to check this.

The cell unit with brass bulbs had a relaxation time of 12 hours for the system He-Ar[3]. Thus under identical conditions the relaxation time for the system Xe-N_2, using equation 4.1, should be given by the following expression.

$$\tau_{Xe\text{-}N_2} = \tau_{He\text{-}Ar}\left[\left(nD_{12}\right)_{He\text{-}Ar} \Big/ \left(nD_{12}\right)_{Xe\text{-}N_2}\right] \qquad (4.2)$$

From equation (4.2) it is apparent that some mean diffusion coefficient is required and although the temperature, $\overline{T}_D$, to which the diffusion coefficient applies is not generally the same as the $\overline{T}$ appropriate to α_T[7], it is taken as so for the purposes of this discussion.

The values of D^0_{12} at 300K for He-Ar[8] and Xe-N_2 (Chapter VII) are given in table 4.2 and equation (4.2) predicts a relaxation time of approximately 67 hours for the Xe-N_2 system.

Table 4.2

Limiting Diffusion Coefficients at 300K.

	D^0_{12}
He-Ar	0.6344
Xe-N_2	0.1317

The determination of α_T as a function of time in the 'new' cell unit is given in table 4.3; the corrections to α_T were made using the experimentally determined concentration dependency of α_T given in chapter VII.

Table 4.3

Variation of α_T with time for Xe-N_2

Time (hours)	α_T corrected to $x_1 = 0.2$
24.6	0.158
32.4	0.167
49.0	0.172
73.6	0.174
95.5	0.173

The data given in Table 4.3 is plotted in Figure 4.3 indicating a relaxation time of approximately 72 hours.

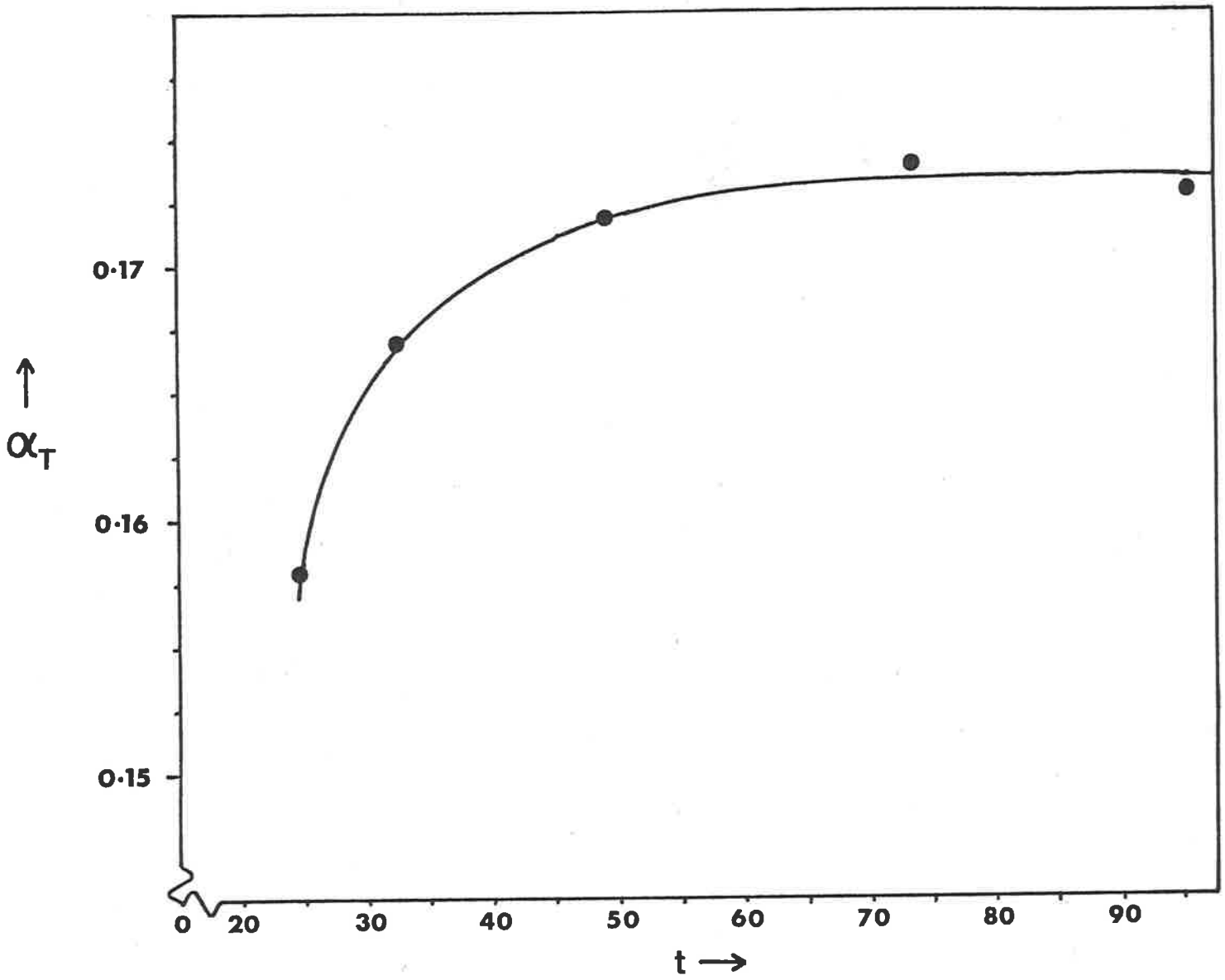

Figure 4.3 Study of the relaxation time of the thermal diffusion cell using Xe-N_2.

Comparison of the projected relaxation time using the cell unit with brass bulbs and the relaxation time measured in the cell unit with stainless steel bulbs, used here, show a deviation of approximately 7%.

The relaxation time of subsequent systems in this study was predicted using equation (4.1) with Xe-N_2 as the base system and the temperature used for the D_{12} values was that temperature to which the experimentally determined value of α_T, was assigned.

REFERENCES

1. M.A. Yabsley and P.J. Dunlop, *Physica* 85A 160 (1976).
2. J. McG. Hall, *Report of the Gravitational Stations in the Metropolitan Area and Salisbury*, South Australian Dept. of mines, Report 58/59 (1964).
3. R.D. Trengove, H.L. Robjohns, T.N. Bell, M.L. Martin and P.J. Dunlop, *Physica* 108A 488 (1981).
4. R.D. Trengove, H.L. Robjohns, M.L. Martin and P.J. Dunlop, *Physica* 108A 502 (1981).
5. R.C. Jones and W.H. Furry, *Rev.Mod.Phys.* 18 151 (1946).
6. K.E. Grew and T.L. Ibbs, *Thermal Diffusion in Gases*, Cambridge University Press, London (1952).
7. E.A. Mason, R.J. Munn and F.J. Smith, *Advances in Atomic and Molecular Physics*, Vol.2, Academic Press, New York (1966).
8. P.S. Arora, H.L. Robjohns and P.J. Dunlop, *Physica* 95A 561 (1979).

CHAPTER V

CONCENTRATION ANALYSIS

5.1 *Introduction*

Thermistors have been used to monitor concentration changes in the determination of both transport properties. A thermistor is a semiconductor device whose resistance is very sensitive to temperature, its temperature coefficient being large and negative. The general properties of thermistors are described adequately elsewhere[1] and will not be repeated here.

It is the self-heating effect of thermistors that makes them highly suitable for monitoring changes in environmental conditions. When sufficient current passes through the thermistor to raise its temperature above the ambient value, its resistance falls, thereby permitting more current to pass and heating the thermistor further, which unless the current is limited by putting a suitable resistor in series, may destroy it. Eventually the thermistor assumes a final resistance corresponding to its steady state temperature, which depends upon the rate at which the heat generated in the thermistor is dissipated. This is influenced to a large extent by the thermal conductivity of the surrounding gas; the other mechanisms for heat dissipation may be controlled by suitable design of the thermistor assembly. Convection is minimised by making the thermistor as small as possible and conduction by the leads is kept to a minimum by making them as fine as practicable.

Since different gases generally have different thermal conductivities they can be discriminated in principle by measuring the resistance of the thermistor in each gas.

5.2 *Diffusion*

The advantage of using thermistors to monitor diffusion is that gas does not have to be removed from the system for analysis. Also thermistors respond quickly to changes in concentration by virtue of their sensitivity to the thermal conductivity of their surroundings.

Van Heijningen et al[2,3] obtained accurate results using thermistors to monitor diffusion and more recently improved techniques have enabled other workers[4-22] to measure D_{12} values to a precision of better than 0.2%.

As the analysis method used in this study has been given in detail previously[4,13,23,24] only a brief outline will be given here.

The Loschmidt cell working equation[4,13] replaces equation (3.11) when the two-bulb cell is used in the *'calibration mode'* (section 3.3). Thus the variation in composition with time at the thermistors is given by

$$\Delta C(t) = A\exp(-t/\tau) \qquad (5.1)$$

where

$$\tau = L^2/\Pi^2 D_{12} \qquad (5.2)$$

Here A is a constant and L is the pseudo cell *'length'* whose value is set by the calibration of the two-bulb cell with Loschmidt data.

It has been shown analytically[13,23,24] that the difference in resistance of the two thermistors in a cell is proportional to the

difference in composition at the thermistors. Hence equation (5.1) may be expressed as

$$F(t) \equiv \Delta R(t) - \Delta R(\infty) = A' \exp(-t/\tau) \qquad (5.3)$$

where $\Delta R(t)$ is the difference in resistance of the two thermistors at time t, $\Delta R(\infty)$ is the residual resistance due to mismatching of the thermistors, A' is a constant and τ is defined in equation (5.2).

The thermistors were connected as two of the arms of a Wheatstone bridge, the other two arms being 5000Ω micacard resistors. A constant potential difference, V, is applied to the bridge as shown in Figure 5.1 and the analysis of the circuit[13] shows that

$$\Delta R(t) = \frac{R_3 V V_{24}}{V_{14}(V_{14}-V_{24})} \qquad (5.4)$$

when the voltages V_{14} and V_{24} are measured simultaneously, at regular time intervals.

During an experiment both output voltages were connected to separate channels of an analogue scanner, which in turn is connected to a digital voltmeter (Solartron, Schlumberger). A crystal timer designed to produce a pulse at preset time intervals, initiates a scan and the output voltages are almost simultaneously transmitted from the digital voltmeter via a remote interface to a 200UT memory bank. Since V_{14} changes slowly with time, negligible error is incurred by recording its value immediately after voltage V_{24}.

The results of the bridge circuit are fitted by the method of least squares[25] to the function given in equation (5.3) to obtain

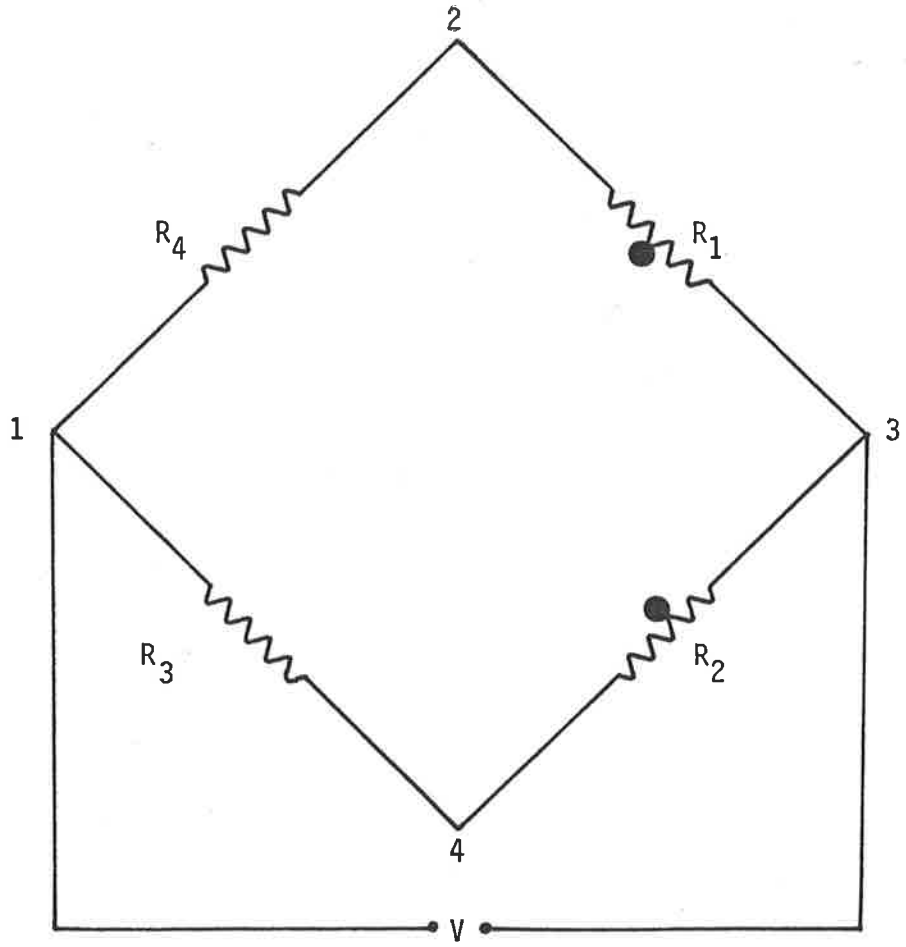

Figure 5.1 The Wheatstone Bridge circuit used for monitoring concentration changes due to diffusion.

D_{12}. Since D_{12} varies approximately inversely with pressure it is convenient for comparison purposes to calculate the more slowly-varying product pD_{12} which is numerically equal to the value of D_{12} 'corrected' to 1 atmosphere pressure if p is expressed in atmospheres.

5.3 *Thermal Diffusion - Thermal Conductivity Cell*

All analyses were performed with a thermal conductivity cell machined from a cylindrical brass block of mass 10kg. Two cavities of equal volume were machined from the block and brass end plates bolted into position, with lead o-rings, sealed the cavities. Each cavity contained one of a set of Fenwal thermistors with nominal resistances of 8kΩ at 298K, which formed two of the arms of a simple Wheatstone bridge identical to that in Figure 5.1.

The thermal conductivity cell, the cavities of which were independently isolated using Nupro bellows valves, was connected via stainless steel tubing to a vacuum system, calibration mixtures, a pressure measurement device and the thermal diffusion cell.

The thermal conductivity cell was suspended vertically in a water bath containing 200l. of water which was controlled to (298±0.002)K by means of a thermistor bridge temperature controller containing an instrumentation operational amplifier Type 725 adjusted for a gain of 300 000.

5.4 *Concentration Determination*

The bath housing the thermal conductivity cell was situated in a room whose temperature was maintained constant to better than

±0.5K for the duration of the analysis procedure by means of an efficient air conditioner.

The contents of the bulbs of the thermal diffusion cell were analysed in combination with the calibration of the thermal conductivity cell using five mixtures of known composition whose preparation is described in section 5.5. All measurements were made in duplicate.

Initial tests with the thermal conductivity cell showed that the absolute values of the resistances of the thermistors were slightly pressure dependent; approximately 1μV/Torr variation in the bridge 'out-of-balance' (V_{24} in Figure 5.1). So the pressures in the thermal conductivity cell were always adjusted to be (125±0.4) Torr by means of a Schlumberger pressure transducer with a digital readout. The pressure transducer was calibrated with a Texas Instruments Bourdon gauge and the calibration had a reproducibility of within 0.1%.

The 'out-of-balance' of the Wheatstone bridge circuit with a given gas mixture was measured with a Hewlett Packard 3490 digital voltmeter interfaced to a HP9810A electronic calculator. All signals were averaged 200 times until three consecutive averages agreed to ±1μV. The duplicate analyses were required to agree to ±3μV.

The 'out-of-balance' voltages corresponding to the given calibration mixtures were least-squared[25] to a parabola to evaluate the constants a, b and c in the equation

$$x_1 = a + bV + c^2V \qquad (5.5)$$

Here x_1 is the mole fraction of the heavy component, and V is the bridge 'out-of-balance' voltage. The composition of the gas in each bulb of the thermal diffusion cell is then determined by inserting

the corresponding 'out-of-balance' voltage into equation (5.5).

In Table 5.1 a typical set of analysis results is shown for an experiment with the system Ne-CO_2 performed at a nominal mole fraction $x_1 = 0.21$. The average thermal diffusion factor was then calculated from equation (3.23) which is repeated here in the convenient form

$$\alpha_T = \ln q / \ln(T'/T) \qquad (5.6)$$

$$q = \frac{x_1 (1-x_1')}{x_1' (1-x_1)} \qquad (5.7)$$

Here a prime on a variable indicates a value corresponding to the higher temperature.

5.5 *Calibration Mixtures*

The calibration mixtures were prepared by pressure in five 1.0 litre stainless steel cylinders immersed in a thermostat bath controlled at (300±0.002)K. The five cylinders had a common manifold and each could be isolated by means of a ¼ inch nupro bellows valve.

Pressure measurements were made using a Texas Instruments Bourdon-Tube gauge fitted with a 506 kPa quartz spiral. The gauge had been calibrated against a dead weight tester (Bell and Howell, type 6-201-0001 primary pressure standard) in this laboratory as described in section 4.2; the reproducibility of the calibration was within 0.03%.

The calibration mixtures covered a mole fraction range of 0.04 to 0.12, depending on the relative thermal conductivities

Table 5.1

Typical calibration of the thermal conductivity cell and the analysis of the bulbs of the thermal diffusion cell.

($Ne-CO_2$; $T'=328.45$; $T=274.95$)

Bottle No.	Bridge reading (mV)	x_1 (calibration)	x_1 (least-square)	δx_1 ($\times 10^4$)
1	-2.168	0.2200_9	0.2200_9	0.0
2	-0.380	0.2100_6	0.2100_7	0.1
3	1.413	0.1999_6	0.1999_3	-0.3
4	3.157	0.1899_7	0.1900_0	0.3
5	4.886	0.1800_9	0.1800_8	-0.1
Top bulb	0.202		0.2067_9	
Bottom bulb	-0.839		0.2126_5	

of the two gases, thereby obtaining an 'out-of-balance' range of greater than 5mV using the circuit described in sections 5.3 and 5.4.

For a mixture with nominal mole fraction, x_i, the pressure of the first component, P_i, required with a final pressure, P_{ij}, was determined from the equations

$$P_i = \frac{(1 + B_m(x_i)P_{ij})}{x_i P_{ij}} - B_{ii} \qquad (5.8)$$

$$B_m(x_i) = (x_i)^2 B_{ii} + 2x_i x_j B_{ij} + (x_j)^2 B_{jj} \qquad (5.9)$$

The pressure virial coefficients, B,[26-31] are at 300K in atm^{-1} and the required counter readings for P_i and P_{ij} were calculated from the calibration data.

To prepare a set of mixtures, the unit of cylinders connected to a stainless steel manifold containing a vacuum system, the Bourdon-gauge and gas cylinders, were first evacuated to give a leak rate better than 1×10^{-4} Torr/min. The first gas was introduced into the calibration vessels to the required pressures with each cylinder successively isolated after attainment of thermal equilibrium. With all five cylinders isolated the manifold was evacuated and then washed three times with the second gas before pumping for ten minutes. The second gas was then introduced into the manifold to a pressure greater than that in any of the cylinders and the cylinders continually 'topped-up' until the required final pressure was attained. The cylinders were then 'topped-up' again after five hours and a further two hours.

The true mole fraction, x_i'', in the cylinders were calculated from the experimental pressures P_i and P_{ij} and the nominal mole fraction, x_i, by iteration from the equation

$$x_i'' = \frac{P_i}{P_{ij}} \left[\frac{(1 + B_m(x_i)P_{ij})}{(1 + B_{ii}P_i)} \right] \quad . \qquad (5.10)$$

REFERENCES

1. *'Thermistor Manual'*, Fenwal Electronics, Framingham, Massachusetts.
2. R.R.J. van Heijningen, A. Feberwee, A. van Oosten and J.J.M. Beenakker, *Physica* 32 1649 (1966).
3. R.R.J. van Heijningen, J.P. Harpe and J.J.M. Beenakker, *Physica* 38 1 (1968).
4. P.J. Carson, P.J. Dunlop and T.N. Bell, *J.Chem.Phys.* 56 531 (1972).
5. M.A. Yabsley and P.J. Dunlop, *Phys.Letters* 38A 247 (1972).
6. K.R. Harris, T.N. Bell and P.J. Dunlop, *Canad.J.Chem.* 50 1874 (1972).
7. K.R. Harris, T.N. Bell and P.J. Dunlop, *Canad.J.Phys.* 50 1644 (1972).
8. P.J. Carson and P.J. Dunlop, *Chem.Phys.Lett.* 14 377 (1972).
9. P.J. Carson, M.A. Yabsley and P.J. Dunlop, *Chem.Phys.Lett.* 15 436 (1972).
10. G.R. Staker, M.A. Yabsley, J.M. Symons and P.J. Dunlop, *J.Chem.Soc., Faraday Trans.I* 70 825 (1974).
11. K.R. Harris and T.N. Bell, *Canad.J.Phys.* 51 2101 (1973).
12. G.R. Staker, P.J. Dunlop, K.R. Harris and T.N. Bell, *Chem.Phys. Lett.* 32 561 (1975).
13. M.A. Yabsley and P.J. Dunlop, *J.Phys.E:Sci.Instru.* 8 834 (1975)
14. G.R. Staker and P.J. Dunlop, *Chem.Phys.Lett.* 42 419 (1976).
15. T.N. Bell, I.R. Shankland and P.J. Dunlop, *Chem.Phys.Lett.* 45 445 (1976).
16. P.S. Arora, I.R. Shankland, M.A. Yabsley, T.N. Bell and P.J. Dunlop, *Rev.Sci.Instrum.* 48 673 (1977).

17. P.S. Arora, P.J. Carson and P.J. Dunlop, *Chem.Phys.Lett.* 54 117 (1978).

18. P.S. Arora, H.L. Robjohns, I.R. Shankland and P.J. Dunlop, *Chem.Phys.Lett.* 59 478 (1978).

19. P.S. Arora, H.L. Robjohns and P.J. Dunlop, *Physica* 95A 561 (1979).

20. P.S. Arora and P.J. Dunlop, *J.Chem.Phys.* 71 2430 (1979).

21. P.S. Arora, H.L. Robjohns, T.N. Bell and P.J. Dunlop, *Aust.J.Chem.* 33 1993 (1980).

22. H.L. Robjohns and P.J. Dunlop, *Ber.Bunsenges Phys.Chem.* 85 655 (1981).

23. M.A. Yabsley, *Ph.D. Thesis,* University of Adelaide (1975).

24. G.R. Staker, *Ph.D. Thesis,* University of Adelaide (1976).

25. J.R. Wolberg, *Prediction Analysis,* Van Nostrand Co.Ltd., Princeton, New Jersey.

26. J. Brewer, *Determination of Mixed Virial Coefficients,* Report No. MRL-2915-C, Airforce Office of Scientific Research, No. 67-2795 (1967).

27. J.H. Dymond and E.B. Smith, *The Virial Coefficients of Pure Gases and Mixtures,* Oxford University Press, Oxford (1980).

28. G.M. Kramer and J.G. Miller, *J.Phys.Chem.* 61 785 (1957)

29. M.L. Martin, R.D. Trengove, K.R. Harris and P.J. Dunlop, *Aust.J.Chem.* 35 1525 (1982).

30. J. Brewer and G.W. Vaughn, *J.Chem.Phys.* 50 2960 (1969).

31. J.H. Dymond and E.B. Smith, *The Virial Coefficients of Gases,* Clarendon Press, Oxford (1969).

CHAPTER VI

EXPERIMENTAL ACCURACY

6.1 *Diffusion - Introduction*

The uncertainty in the diffusion coefficient resulting from any uncertainty in the experimental quantities used in its calculation can be estimated by differentiating equation (5.3); resulting in the following relationship.

$$\left| \frac{dD_{12}}{D_{12}} \right| \leq 2 \left| \frac{dL}{L} \right| + \left| \frac{dt}{t} \right| + \frac{L^2}{\pi D_{12} t} \left| \frac{dF(t)}{F(t)} \right| \qquad (6.1)$$

Sources of error such as the Dufour effect, heat-of-mixing and the concentration dependence of diffusion are more difficult to determine and are dealt with in a more general way.

6.2 *Errors in L and t*

The length, L, used in calculating D_{12} is the pseudo 'length' assigned via the calibration with Loschmidt data, this having a maximum uncertainty of 0.2%. As the quantity L^2 is determined by the calibration the maximum uncertainty in L is 0.1%. Thus from equation (6.1) the uncertainty in D_{12} due to any uncertainty in L is 0.2%.

The error in t comes from three sources,

(i) variation in Δt for data collection;

(ii) lag time due to the response time of the scanner and digital voltmeter; and

(iii) any uncertainty in commencement of the experiment. The crystal

timer initiating the scan has an accuracy of 0.01% leading to an error in t of 0.01%. The combined response times of the scanner and digital voltmeter are approximately 100 msec which will be constant for all data points with the result that the commencement of data collection will be uncertain by less than 0.01%. To start an experiment a tap at one end of the two-bulb cell is opened, leading to an uncertainty of the order of a second in the time at which the experiment starts. Tests in the laboratory show that errors of this magnitude result in negligible uncertainty in the value of D_{12}.

6.3 *Errors in* F(t)

Errors in F(t) result from uncertainties in the voltages to calculate $\Delta R(t)$ and $\Delta R(\infty)$. The accuracy of the digital voltmeter and constant power supply used result in an uncertainty in F(t) of approximately 0.3%. The term, $L^2/\pi D_{12}t$, associated with F(t) in equation (6.1) has a maximum value of 0.7 for the experiments in this study. So the uncertainty in D_{12} resulting from uncertainty in F(t) will be approximately 0.2%.

6.4 *Pressure and Temperature*

The temperature of the thermostat bath could be measured within ±0.002K and during the diffusion period the temperature variations were never greater than ±0.002K. In view of the temperature control any convection within the cell would be negligible and thus any resultant inaccuracy in D_{12} due to temperature variation is negligible.

Pressure measurements were accurate to approximately 0.04% and the calibration of the pressure gauge indicates a reproducibility

in the gauge reading of within 0.03%.

Non-ideality and kinetic phenomena may cause deviations from isothermal and isobaric conditions. The heat-of-mixing and Dufour effect are two such effects that will disturb the temperature of a diffusing gas.

The heat-of-mixing is due to the real nature of the gas system, and its magnitude is approximately proportional to the product x_1x_2P[1] and thus may be reduced by choice of suitable experimental conditions. Martin et al[2] working at 200kPa have estimated the heat-of-mixing for some of the systems studied here, showing it to be rather small at the pressures used in this study. Also the heat-of-mixing decays at three times the relaxation due to diffusion[3] and thus should become negligible after a period of time. The Dufour effect refers to the transient temperature difference produced by a concentration gradient and is regarded as the inverse of thermal diffusion. In general, the magnitude of the temperature difference is small when the component masses are comparable[4,5] and decays at approximately the same rate as diffusion.[3] If the cross-sectional area of the cell is small the temperature gradients are rapidly dissipated by conduction to the cell walls. Both of these effects exist in the two-bulb apparatus but as diffusion is mainly confined to the 'inserts' any transient heat generated will be dissipated before reaching the thermistors and thus should not interfere with the diffusion process.

A pressure gradient may arise during diffusion because of a difference in the average molecular velocities, but such gradients are negligible except in the case of diffusion within a capillary.[6]

6.5 *Concentration Dependent Diffusion*

As yet, no analytical solution exists to Fick's second law for concentration dependent diffusion,

$$(\partial C_i/\partial t) = D_{12}(\partial^2 C_i/\partial z^2) + (\partial D_{12}/\partial C_i)(\partial C_i/\partial z)^2 \quad (6.2)$$

This has led to the use of approximations which reduce the magnitude of the second term of equation (6.2) with respect to the first. Ljunggren[7] has shown that in the case where D_{12} is a linear function of concentration the diffusion coefficient may be considered constant with a value corresponding to that of the mean concentration of the experiment. Thus the simplest form of Fick's second law may be assumed.

In this study only differential composition differences existed between the two bulbs of the diffusion cell and therefore it is reasonable to assume that the result of Ljunggren applies and the simple form of equation (6.2) may be used.

6.6 *Comparison with Loschmidt results above and below 300K.*

The two-bulb cell has been calibrated with Loschmidt data at 300K. The results obtained with the two-bulb cell have been compared with Loschmidt data 25K either side of the calibration temperature for the system Ar-O_2.[8,9] The two sets of results agree to within 0.1%.

In summary, the accumulation of those errors that have been estimated numerically in the foregoing discussion gives rise to a possible maximum uncertainty of ±0.5% in D_{12}. This compares favourably

with the average experimental precision of ±0.1%.

6.7 *Thermal Diffusion - Introduction*

The uncertainty in α_T resulting from the uncertainty in any of the quantities used to calculate it can be quite readily estimated by differentiating equations (5.6) and (5.7).

$$\left|\frac{d\alpha_T}{\alpha_T}\right| \leq \frac{1}{\alpha_T}\left[\left|\frac{dx_1}{x_1}\right| + \left|\frac{dx_1'}{x_1'}\right| + \left|\frac{d(1-x_1')}{(1-x_1')}\right| + \left|\frac{d(1-x_1)}{(1-x_1)}\right|\right] + \frac{1}{\alpha_T}\left[\left|\frac{dT'}{T'}\right| + \left|\frac{dT}{T}\right|\right] \quad . \qquad (6.3)$$

The uncertainty in α_T resulting from its concentration and temperature dependence and any uncertainty in the composition of the calibration mixtures are discussed analytically.

6.8 *Errors in* T, T' *and* x_1, x_1'.

The temperatures of the two refrigerated baths used for thermal diffusion experiments were controlled to ±0.02K by means of thermistor bridge temperature controllers. The resulting uncertainty in α_T, calculated for the smallest value of α_T measured in this study, is 0.3%. For experiments with $\overline{T}$ equal to 300K or above, one or both of the baths were used without the refrigeration unit and the temperature controlled to ±0.002K; thus the resulting uncertainty will be much less than the value stated above.

The values of x_1 and x_1' are determined by interpolation from the least-squaring of the known composition of the calibration mixtures

against their respective bridge 'out-of-balances'. The sources of error in the values of x_1 and x_1' are uncertainty in the composition of the calibration mixtures, which is considered in section 6.8, error in the bridge 'out-of-balance' and agreement between duplicate measurements in the analysis procedure.

The digital voltmeter readings are signal averaged to remove the influence of external electrical noise, but the digital voltmeter has a precision of $\pm 2\mu V$. This results in a maximum uncertainty in the mole fractions x_1 and x_1' of 3×10^{-5}; this figure is calculated from the worst bridge resolution (or out-of-balance range) encountered in this study and for most experiments this is less than 1.5×10^{-5} but the higher value is used. The resolution obtainable with the bridge circuit is a result of the relative thermal conductivities of the component gases.

The degree of agreement between duplicate measurements in the analysis procedure results in further uncertainty in the values of x_1 and x_1'. The worst agreement between duplicate measurements for a given analysis when combined with the resolution of the bridge circuit allow uncertainty in x_1 and x_1' from this source to be readily calculated. As this must be determined for each individual experiment it is given as part of the total error with the tabulated α_T values in Appendix IV.

6.9 *Calibration mixtures*

The estimated accuracy of pressure measurements is 0.04% and the calibration of the pressure gauge is reproducible to within

0.03%. The drift in the zero of the pressure gauge was less than 7 counter divisions over 24 hours which is less than 0.01% of the final pressure used in preparation of the mixtures.

The errors in the second virial coefficients used in gauge predictions and calculation of the mole fractions were as great as 0.8×10^{-4} atm^{-1}. This results in errors of approximately 0.2% in the mole fractions of the calibration mixtures.

Calculations showed that the uncertainties in the calibration mixtures were not reflected in α_T. As the uncertainties are essentially the same for each individual mixture any systematic errors cancelled because the thermal diffusion factor depends on the *ratio* of the mole fractions in the two bulbs.

6.10 *Concentration and Temperature Dependent Thermal Diffusion*

To examine the effects of the concentration and temperature dependence of the thermal diffusion on the experimental values, α_T is expanded in a Taylor series about the point $(\bar{x}, \bar{T})$

$$\alpha_T = \alpha^0 + D_1(x_1 - \bar{x}_1) + D_2(T - \bar{T}) + \ldots \quad (6.4)$$

$$= \alpha^0[1 + R_1(x_1 - \bar{x}_1) + R_2(T - \bar{T}) + \ldots] \quad (6.5)$$

$$R_1 = \frac{1}{\alpha^0}\left(\frac{\partial \alpha_T}{\partial x_1}\right)_{\bar{x}_1, \bar{T}} \quad (6.6)$$

$$R_2 = \frac{1}{\alpha^0}\left(\frac{\partial \alpha_T}{\partial T}\right)_{\bar{x}_1, \bar{T}} \quad (6.7)$$

$$\alpha^0 = \alpha_T(\bar{x}_1, \bar{T}) \quad (6.8)$$

Then the above expansions are substituted into the basic differential equation for thermal diffusion[10,11]

$$\frac{dx_1}{dz} = -\alpha_T(1-x_1)x_1 \frac{d\ \ln T}{dz} \qquad (6.9)$$

and equation (6.9) integrated between the limits (x_1, T) for the cold bulb and (x_1', T') for the hot bulb of the cell. This results in the following relations

$$\alpha_T(\bar{x}_1, \bar{T}) = \alpha_T^{exp} + \Delta_1 + \Delta_2 \qquad (6.10)$$

$$\alpha_T^{exp} = \ln[(x_1/x_1')\ ((1-x_1')/(1-x_1))]/[\ln(T'/T)] \qquad (6.11)$$

$$\Delta_1 = [\ln(T'/T)]^{-1}\ [A \ln (x_1/x_1') + B \ln [(1-x_1)/(1-x_1')] + C \ln [(1+aR_1x_1)/(1+aR_1x_1')]] \qquad (6.12)$$

$$\Delta_2 = \alpha^0 R_2[\bar{T}-[(T'-T)/\ln (T'/T)]] \qquad (6.13)$$

The derivation of equation (6.10) and terms contained therein are given in Appendix II. The term Δ_1 in equation (6.10) is the concentration dependence correction term and Δ_2 is the temperature dependence correction term.

The term Δ_1 has been calculated for the systems He-Ar, He-SF_6 and H_2-Xe using experimental values[12,13] for the variables in equation (6.12). These calculations show that the term Δ_1 is less than 0.1% of α_T.

Inspection of equation (6.13) shows that the magnitude of the term Δ_2 is largely dependent on the difference $\bar{T}-[(T'-T)/\ln (T'/T)]$. α_T values have been calculated to the third Chapman-Cowling approximation[14] at several temperatures for the system N_2-Xe using the (*m*68) potential given in Chapter VII. The results are given in Tables 6.1 and 6.2 for

$x_1 = 0.2$ and $x_1 = 0.8$ respectively and they show that α_T is a linear function of temperature over 50K. Using this temperature dependence the derivation of Brown[15,16] can be used to show that the value of α_T^{exp} corresponds to a temperature given by[17]

$$\bar{T} = (T' - T)/\ln (T'/T) \qquad (6.14)$$

Thus if α_T is assumed to be linearly dependent on the absolute temperature the term Δ_2 is always zero.

In summary, the accumulation of those errors that have been numerically estimated in the foregoing discussion gives rise to a possible maximum uncertainty of 0.4% in α_T. To be added to this is the major portion due to the resolution of the bridge circuit and agreement between duplicate measurements in the analysis procedure.

Table 6.1

Linearity of α_T with Temperature

(α_T values calculated for the third Chapman-Cowling approximation for the (15,6,8,γ = 0.8) potential function ($Xe-N_2$) are least-squared as a function of temperature for x_1 = 0.2)

T(K)	$(\alpha_T)_{theory}$	$(\alpha_T)_{least\text{-}square}$	$\delta\%$
250	0.145_2	0.145_0	-0.1_4
260	0.152_3	0.152_2	-0.0_7
270	0.159_2	0.159_4	$+0.1_3$
275	0.162_8	0.162_9	$+0.0_6$
280	0.166_4	0.166_5	$+0.0_6$
290	0.173_7	0.173_7	0.0_0
300	0.181_0	0.180_8	-0.1_1

$$\alpha_T = -0.033_8 + 7.15_4 \times 10^{-4} T$$

The average deviation is $\pm 0.0_8\%$.

Table 6.2

Linearity of α_T with Temperature

(α_T values calculated for the third Chapman-Cowling approximation for the (15,6,8,γ = 0.8) potential function ($Xe-N_2$) are least-squared as a function of temperature for x_1 = 0.8).

T(K)	$(\alpha_T)_{theory}$	$(\alpha_T)_{least\text{-}square}$	$\delta\%$
250	0.104_5	0.104_4	-0.1_0
260	0.109_7	0.109_6	-0.0_9
270	0.114_7	0.114_8	$+0.0_9$
275	0.117_3	0.117_4	$+0.0_9$
280	0.119_9	0.120_0	$+0.0_8$
290	0.125_2	0.125_2	0.0_0
300	0.130_5	0.130_4	-0.0_8

$$\alpha_T = -0.025_5 + 5.19_6 \times 10^{-4}\ T$$

The average deviation is 0.0_8%.

REFERENCES

1. M. Knoester, K.W. Taconis and J.J.M. Beenakker, *Physica* 33 389 (1967).
2. M.L. Martin, R.D. Trengove, K.R. Harris and P.J. Dunlop, *Aust.J.Chem.* 35 1525 (1982).
3. M.A. Yabsley, *Ph.D. Thesis*, University of Adelaide (1975).
4. K. Clusius and L. Waldman, *Die Naturwiss.* 30 711 (1942).
5. L. Miller, *Z. Naturforsch.* 4a 262 (1949).
6. K.P. McCarty and E.A. Mason, *Phys.Fluids* 3 908 (1960).
7. S. Ljunggren, *Ark.Kemi.* 24 1 (1965).
8. P.S. Arora, H.L. Robjohns, T.N. Bell and P.J. Dunlop, *Aust.J.Chem.* 33 1993 (1980).
9. P.J. Dunlop, *Private Communication.*
10. E.A. Mason, R.J. Munn, and R.J. Smith, *Advances in Atomic and Molecular Physics*, Vol. 2, p. 37, Academic Press (1966).
11. G.C. Maitland, M. Rigby, E.B. Smith and W.A. Wakeham, *Intermolecular Forces*, p. 354, Oxford University Press (1981).
12. R.D. Trengove, H.L. Robjohns, T.N. Bell, M.L. Martin and P.J. Dunlop, *Physica* 108A 488 (1981).
13. R.D. Trengove, H.L. Robjohns, M.L. Martin and P.J. Dunlop, *Physica* 108A 502 (1981).
14. E.A. Mason, *J.Chem.Phys.* 27 75 (1957).
15. H. Brown, *Phys.Rev.* 58 661 (1940).
16. K.E. Grew and T.L. Ibbs, *Thermal Diffusion in Gases*, p. 126, Cambridge University Press (1952).
17. R. Paul, A.J. Howard and W.W. Watson, *J.Chem.Phys*, 43 1622 (1965).

CHAPTER VII

EXPERIMENTAL RESULTS AND DISCUSSION

7.1 *Introduction*

The results for individual diffusion experiments are tabulated in Appendix III (Tables III.2 to III.19); the insert used for studying each system, characterised by the internal diameter, is listed in Table III.1. The results of individual thermal diffusion experiments are tabulated in Appendix IV (Tables IV.3 to IV.9); the second virial coefficients required for calculation of calibration mixture compositions are listed in Tables IV.1 and IV.2.

The constants, obtained from least squaring of the experimental data, summarising the concentration and temperature dependencies of the transport properties are presented in sections 7.2 to 7.4.

The parameters for the potential energy functions derived from the diffusion data in combination with second virial coefficients in the literature, using the method outlined in section 2.3, are presented in section 7.5.

The experimental data are used to test the potentials obtained as part of this study as well as potentials in the literature, and compared with experimental results of other workers, in section 7.6.

7.2 *Concentration Dependence of Diffusion*

All experimental values of D_{12} given in Appendix III are values corrected to one atmosphere pressure, $(D_{12})_{p=1}$.

The experimental values for each system at 300K have been fitted to the *empirical* relation

$$D_{12} = D_{12}^{0} \quad (1 + \frac{a_1 x_1}{1 + a_2 x_1}) \qquad (7.1)$$

where a_1 and a_2 are constants. The form of equation (7.1) was first suggested by Adamur and Schatzki[1] and later by Mason and Marrero.[2] Yabsley, Carson and Dunlop[3] have shown that it reproduces the form of the concentration dependence of D_{12} predicted by the Chapman-Enskog theory.[4,5]

The values of D_{12}^{0}, a_1 and a_2 determined for each system, together with the average percentage deviation ($\delta\%$) of the experimental points from the smooth curve, are given in Tables 7.1 to 7.4. The concentration dependencies of the systems He-N_2 and Ar-N_2[6] and of the Rare Gas-CH_4 systems[6,7,8] are also given for completeness.

The diffusion coefficients in the tables that follow have the units cm^2/s^{-1}.

Table 7.1

Concentration Dependence of D_{12} at 300K for the Rare Gas - Hydrogen Systems

	D^0_{12}	a_1	a_2	$\delta\%$
Ne-H_2	1.176_5	0.0773	1.0695	±0.05
Ar-H_2	0.824_0	0.0538	1.2193	±0.02
Kr-H_2	0.724_0	0.0577	1.6003	±0.03
Xe-H_2	0.623_3	0.0665	1.2689	±0.06

Table 7.2

Concentration Dependence of D_{12} at 300K for the Rare Gas - Deuterium Systems

	D^0_{12}	a_1	a_2	$\delta\%$
Ne-D_2	0.871_3	0.0421	0.8133	±0.05
Ar-D_2	0.549_2	0.0723	1.9456	±0.04
Kr-D_2	0.518_2	0.0270	0.4908	±0.05
Xe-D_2	0.446_5	0.0262	1.2125	±0.06

Table 7.3[a]

Concentration Dependence of D_{12} at 300K for the Rare Gas - Nitrogen Systems

	D^0_{12}	a_1	a_2	$\delta\%$
He-N_2	0.706_7	0.0675	1.4883	±0.04
Ne-N_2	0.339_8	-	-	±0.03
Ar-N_2	0.203_4	0.0041	-	±0.04
Kr-N_2	0.159_5	0.0058	-	±0.02
Xe-N_2	0.131_7	0.0064	-	±0.08

[a] The results for He-N_2 and Ar-N_2 are those of Arora et al.[6]

Table 7.4[a]

Concentration Dependence of D_{12} at 300K for the Rare Gas - Methane Systems

	D^0_{12}	a_1	a_2	$\delta\%$
He-CH_4	0.680_2	0.0457	1.5110	±0.04
Ne-CH_4	0.356_8	0.0018	-	±0.02
Ar-CH_4	0.219_6	0.0190	1.3787	±0.02
Kr-CH_4	0.178_6	0.0008	-	±0.02
Xe-CH_4	0.148_1	0.0128	-	±0.03

[a] The data in this table are those of Dunlop and co-workers.[6,7,8]

7.3 *Temperature Dependence of Diffusion*

Diffusion coefficients were measured from 277 to 323K and, as the Chapman-Enskog theory for binary diffusion indicates that, over a range of 50K, the *variation* in the concentration dependence of D_{12} is less than 0.1%,[9] the concentration dependencies described by equation (7.1) and Tables 7.1 to 7.4 were used to extrapolate the experimental D_{12} values at each temperature to $x_1 = 0$. The values of $\overset{0}{D}_{12}$ obtained in this way were fitted to polynomials in the temperature

$$\overset{0}{D}_{12} = b_0 + b_1 T + b_2 T^2 \quad . \qquad (7.2)$$

The values of b_0, b_1 and b_2 determined for each binary system are given in Tables 7.5 to 7.7. The term $\delta\%$ in the tables is the average of the percentage deviations of the experimental points from the smooth curves.

In addition to fitting the $\overset{0}{D}_{12}$ values to polynomials in temperature the functions

$$\overset{0}{D}_{12} = b_0 e^{b_1 T} \qquad (7.3)$$

and

$$\overset{0}{D}_{12} = b_0 T^{b_1} \qquad (7.4)$$

were tested. For mixtures of the rare gases with nitrogen equation (7.3) gave average deviations which were twice the experimental precision whilst equation (7.4) gave deviations comparable to equation (7.2). However for other systems studied in this laboratory neither equation (7.3) or (7.4) were able to reproduce the $\overset{0}{D}_{12}$ values within the experimental precision.

Table 7.5

Temperature Dependence of D_{12}^{0} for the Rare Gas - Hydrogen Systems

	$b_0 \times 10$	$b_1 \times 10^3$	$b_2 \times 10^6$	δ%
Ne-H_2	-0.6268	1.6616	8.2189	±0.04
Ar-H_2	0.2656	0.5036	7.1737	±0.05
Kr-H_2	-1.1147	1.3241	4.8648	±0.05
Xe-H_2	-0.2719	0.6684	4.9914	±0.08

Table 7.6[a]

Temperature Dependence of D_{12}^{0} for the Rare Gas - Nitrogen Systems

	$b_0 \times 10^2$	$b_1 \times 10^4$	$b_2 \times 10^6$	δ%
He-N_2	-14.8236	17.6579	3.6152	±0.04
Ne-N_2	-9.1510	9.5686	1.6037	±0.03
Ar-N_2	-8.6126	7.1359	0.8375	±0.06
Kr-N_2	-4.2460	3.7360	0.9987	±0.02
Xe-N_2	-0.3067	0.8819	1.2029	±0.02

[a] The temperature dependencies of He-N_2 and Ar-N_2 were reported[6] for $x_1 = 0.2$ and $x_1 = 0.5$ respectively, but the original data was corrected to D_{12}^{0} giving the results above.

Table 7.7[a]

Temperature Dependence of $\overset{0}{D}_{12}$ for the Rare Gas - Methane Systems

	$b_0 \times 10^2$	$b_1 \times 10^4$	$b_2 \times 10^6$	$\delta\%$
He-CH_4	-8.5062	13.0972	4.1352	±0.05
Ne-CH_4	-16.6726	15.8005	0.5491	±0.06
Ar-CH_4	-3.2510	3.7740	1.5525	±0.05
Kr-CH_4	-4.3961	3.6896	1.2438	±0.03
Xe-CH_4	-0.4314	0.8834	1.3999	±0.04

[a] The temperature dependencies above are listed as they were a companion study in this laboratory to the thermal diffusion study.

7.4 *Concentration and Temperature Dependence of Thermal Diffusion.*

When thermal diffusion factors are calculated to the third Chapman-Cowling approximation[5] $(\alpha_T)^{-1}$ is found to be a linear function of x_1 with the maximum deviation from the least-squared line of less than 0.5%. The relationship between $(\alpha_T)^{-1}$ and x_1 was first found experimentally by Laranjeira[10] and results in this laboratory[11] for mixtures of rare gases showed average deviations within the above limit. Thus the results in Appendix IV were used to evaluate for each system the constants c_0 and c_1 in the expression

$$(\alpha_T)^{-1} = c_0 + c_1 x_1 \quad . \qquad (7.5)$$

The constants c_0 and c_1 for each system at each temperature are given in Tables 7.8 to 7.14; the term $\delta\%$ is the average deviation of the experimental values from the least squared time and $\overline{T}$ calculated using equation (3.27) in degrees Kelvin.

Table 7.8

Least-square coefficients for the composition dependence of $(\alpha_T)^{-1}$ for He-Ar.

$\overline{T}$	c_0	c_1	$\delta\%$
255.3	1.436	2.212	±0.2
270.8	1.466	2.146	±0.4

Table 7.9

Least-square coefficients for the composition dependence of $(\alpha_T)^{-1}$ for Ar-Kr.

$\overline{T}$	c_0	c_1	$\delta\%$
255.3	12.915	3.346	±2.1
300.0	9.614	3.588	±2.2

Table 7.10

Least-square coefficients for the composition dependence of $(\alpha_T)^{-1}$ for Rare Gas - Hydrogen Systems

	$\overline{T}$	c_0	c_1	$\delta\%$
Ne-H_2	300.8	2.753	0.874	±0.2
Ar-H_2	300.8	2.112	2.282	±0.5
Kr-H_2	300.8	1.919	2.776	±0.2
Xe-H_2	300.8	1.756	3.119	±0.1

Table 7.11

Least-square coefficients for the composition dependence of $(\alpha_T)^{-1}$ for Rare Gas - Deuterium Systems

	$\bar{T}$	c_0	c_1	$\delta\%$
Ne-D_2	300.9	3.326	0.814	±0.2
Ar-D_2	300.9	2.329	2.341	±0.4
Kr-D_2	300.9	2.037	2.755	±0.3
Xe-D_2	300.9	1.805	3.161	±0.2

Table 7.12

Least-square coefficients for the composition dependence of $(\alpha_T)^{-1}$ for Rare Gas - Nitrogen Systems

	$\bar{T}$	c_0	c_1	$\delta\%$
He-N_2	253.9	1.522	2.387	±0.7
	300.8	1.514	2.379	±0.2
Ne-N_2	255.3	12.480	7.942	±1.2
	270.8	11.526	8.432	±0.3
	300.9	11.066	7.512	±0.3
Ar-N_2	255.3	15.396	-1.562	±0.2
	270.8	14.565	-0.833	±1.5
	300.9	13.472	-0.750	±0.3
Kr-N_2	254.2	8.104	1.089	±0.2
	270.8	7.442	1.609	±0.5
	300.9	6.553	1.366	±0.5
Xe-N_2	253.3	6.856	2.792	±1.6
	274.2	5.986	2.780	±0.3
	300.9	5.243	2.594	±0.2

Table 7.13

Least-square coefficients for the composition dependence of $(\alpha_T)^{-1}$ for $Ne-CO_2$

$\overline{T}$	c_0	c_1	$\delta\%$
270.8	4.230	4.776	±0.6
300.9	4.056	4.647	±0.2
324.3	3.969	4.452	±0.2

Table 7.14

Least-square coefficients for the composition dependence of $(\alpha_T)^{-1}$ for Rare Gas - Methane Systems

	$\overline{T}$	c_0	c_1	$\delta\%$
$He-CH_4$	300.9	1.797	2.839	±0.3
$Ne-CH_4$	300.9	51.00	-27.82	±0.8
$Ar-CH_4$	300.9	9.473	-0.051	±0.6
$Kr-CH_4$	300.9	7.387	2.273	±0.3
$Xe-CH_4$	300.9	7.490	4.220	±0.1

In Chapter 6 and Appendix II α_T was assumed to be linearly dependent on the absolute temperature in the derivation of the temperature correction for the experimental values. Inspection of Tables 6.1 and 6.2 shows that over a temperature range of 50K this is supported theoretically.

Using the coefficients in Tables 7.12 and 7.13 the smoothed experimental results have been used to determine the coefficients d_0 and d_1 in the relationship

$$\alpha_T = d_0 + d_1 T \quad . \qquad (7.6)$$

The coefficients d_0 and d_1 for the systems Ne-CO_2, Kr-N_2 and Xe-N_2 are given in Table 7.15. The deviations of the smoothed experimental results from the least-squared lines (equation 7.6) are shown in Table 7.16. The deviations are all much less than the experimental error and except for Kr-N_2 at x_1 = 0.8 less than 0.4%.

Table 7.15

Least-squared coefficients for the temperature dependence of α_T

	x_1	d_0	$d_1 \times 10^4$
Ne-CO_2	0.2	0.1275	2.418
	0.8	0.0807	1.601
Kr-N_2	0.2	-0.0240	5.662
	0.8	0.0005	4.302
Xe-N_2	0.2	-0.0697	8.091
	0.8	-0.0315	5.586

Table 7.16[a,b,c].

Test of linearity of α_T with absolute temperature.

$Ne-CO_2$

	$\bar{T}$	$(\alpha_T)_{smooth}$	$(\alpha_T)_{least\text{-}square}$
x_1=0.2	270.8	0.1929	0.1930
	300.9	0.2006	0.2003
	324.3	0.2058	0.2060
x_1=0.8	270.8	0.1242	0.1241
	300.9	0.1286	0.1289
	324.3	0.1328	0.1326

$Kr-N_2$

	$\bar{T}$	$(\alpha_T)_{smooth}$	$(\alpha_T)_{least\text{-}square}$
x =0.2	254.2	0.1202	0.1199
	270.8	0.1288	0.1293
	300.9	0.1465	0.1463
x =0.8	254.2	0.1114	0.1099
	270.8	0.1146	0.1170
	300.9	0.1308	0.1299

Xe-N_2

	$\bar{T}$	$(\alpha_T)_{smooth}$	$(\alpha_T)_{least\text{-}square}$
x_1=0.2	253.3	0.1349	0.1353
	274.2	0.1529	0.1522
	300.9	0.1735	0.1738
x_1=0.8	253.3	0.1100	0.1100
	274.2	0.1218	0.1217
	300.9	0.1366	0.1366

a $\bar{T}$ is calculated using equation (3.27)

b $(\alpha_T)_{smooth}$ is the value of α_T calculated using the coefficients in Tables 7.12 and 7.13.

c $(\alpha_T)_{least\text{-}square}$ is the value of α_T calculated using the coefficients in Table 7.15.

7.5 *Potential functions derived using the data from this study.*

Parameters for spherical (m68) potentials were derived using the method outlined in section 2.3. Possible potential functions, characterised by ε_{12} and σ_{12} values, obtained using the experimental diffusion coefficients were differentiated by their ability to reproduce the interaction second virial coefficients from the literature.[12,13,14]

The best potentials resulting from this procedure are given in Tables 7.17 to 7.19. Again the results for He-N_2, Ar-N_2[6] and rare gas - methane mixtures[8] are presented for completeness. Also listed in the tables are the average deviations of the calculated interaction second virial coefficients from the experimental values,[12,13,14] $\delta(B_{12})$, in units of $cm^3\ mol^{-1}$. The units of ε_{12}/k are K and of σ_{12} are Å. The error in the B_{12} values used is estimated to be 1.5-2.0 $cm^3\ mol^{-1}$.

As outlined in Chapter 2 the potentials presented here will only approximate the 'true' intermolecular potential and will certainly not be expected to describe long-range interactions adequately.

Table 7.17[a]

(m68) Potential parameters obtained from diffusion and second virial data for Rare Gas - Hydrogen Systems.

	Potential	ε_{12}/k	σ_{12}	$\delta(B_{12})$
Ne-H_2	10,6,8,γ=2.0	34.0±3.0	2.858±0.010	2.5
Ar-H_2	12,6,8,γ=2.5	97.0±3.0	2.986±0.010	2.3
Kr-H_2	11,6,8,γ=3.0	101.0±3.0	3.159±0.010	1.8
Xe-H_2	11,6,8,γ=3.0	106.0±3.0	3.376±0.010	1.1

[a] These potentials were also used to describe the rare gas-deuterium systems.

Table 7.18[a]

(m68) Potential parameters obtained from diffusion and second virial data for Rare Gas - Nitrogen Systems.

	Potential	ε_{12}/k	σ_{12}	$\delta(B_{12})$
$He-N_2$	11,6,8,γ=0.0	21.0±3.0	3.262±0.010	0.4
$Ne-N_2$	12,6,8,γ=0.5	55.0±3.0	3.164±0.010	0.5
$Ar-N_2$	9,6,8,γ=4.0	99.5±3.0	3.546±0.010	1.4
$Kr-N_2$	15,6,8,γ=0.8	176.0±3.0	3.414±0.010	0.9
$Xe-N_2$	15,6,8,γ=0.8	190.0±3.0	3.622±0.010	1.5

[a] The potentials for $He-N_2$ and $Ar-N_2$ have been reported by this laboratory previously.[6]

Table 7.19[a]

(m68) Potential parameters obtained from diffusion and second virial data for Rare Gas - Methane Systems.

	Potential	ε_{12}/k	σ	$\delta(B_{12})$
He-CH_4	10,6,8,γ=2.0	21.5±3.0	3.402	0.5
Ne-CH_4	20,6,8,γ=0.0	75.0±3.0	3.121	0.5
Ar-CH_4	20,6,8,γ=0.0	190.0±3.0	3.334	1.4
Kr-CH_4	11,6,8,γ=0.25	162.0±3.0	3.655	3.2
Xe-CH_4	13,6,8,γ=2.0	270.0±3.0	3.610	1.0

[a] These potentials have been reported by this laboratory.[6,7,8]

7.6 *Discussion*

The parameters for the potentials used to calculate transport properties for comparisons in this section are given in Appendix V. Table V.1 lists the parameter for *like* interactions and Table V.2 lists the parameters for *unlike* interactions. The spherical potentials used for the like interactions[15-22] are considered to be the best currently available in the literature. The experimental potential of Mason and Rice[19] is used for hydrogen in preference to others with a more theoretical basis[23] as it gives a better representation of the transport properties and the second virial coefficients.

Thermal diffusion factors were measured for the system He-Ar as part of this study primarily for use as a standard system to monitor the performance of the apparatus. The results were also used to test the interaction potential designated as best in a study of rare gas mixtures at 300K,[11] at other temperatures. The experimental values of α_T are compared with values calculated using the potentials,[15,17,24] in Tables V.1 and V.2, in Table 7.20 where the two are seen to be in excellent agreement; the comparison at 300K[11] is also included. The values in Table 7.20 also indicate that over 45K there is no change in α_T within experimental error. Calculations to the third Chapman-Cowling approximation show that in general, systems containing helium exhibit very little variation of α_T with temperature.

Table 7.20[a]

Comparison between smoothed experimental and theoretical thermal diffusion factors for He-Ar

T(K)	x_1	$(\alpha_T^{exp})_{smooth}$	α_T^{th}	δ%
255.3	0.2	0.532	0.527	-1.0
	0.8	0.312	0.308	-1.3
270.8	0.2	0.528	0.530	+0.4
	0.8	0.314	0.310	-1.3
300.8	0.2	0.531	0.533	+0.4
	0.8	0.316	0.313	-1.0

a α_T^{exp} is the experimental thermal diffusion factor, α_T^{th} the theoretical value and δ% the percentage deviation between the two values.

As mixtures of the heavier rare gases were neglected in a study previously carried out in this laboratory,[11] the publication of a new interaction potential for Ar-Kr by Aziz and van Dalen,[25] which predicts the precise diffusion results of Arora et al[26] very well, prompted the study of thermal diffusion for this system.

The experimental values were used to test this potential as well as some existing potential functions in the literature.[27-29] The experimental data are compared with theoretical values calculated to the third Chapman-Cowling approximation, using the potentials in Tables V.1[17,18] and V.2,[25,27-29] in Table 7.21. This comparison shows that almost all the potentials agree within the maximum experimental error, but only the MSMV potential[22] reproduces the experimental results sufficiently well within the experimental precision, given in Table 7.9.

Table 7.21[a,b]

Comparison between smoothed experimental and theoretical thermal diffusion factors for Ar-Kr

$\bar{T}$ (K)	x_1	$(\alpha_T^{exp})_{smooth}$	δ% HFD-C2 (25)	δ% MSMV (27)	δ% MSMSV (28)	δ% MS (29)
255.3	0.2	0.073_6	-2.0	+1.6	-3.8	-5.0
	0.8	0.064_1	-5.3	-1.7	-6.1	-8.7
300.0	0.2	0.096_8	-5.2	-1.6	-6.6	-7.6
	0.8	0.081_0	-4.7	-1.0	-5.1	-7.5

[a] δ% is the percentage deviation between theoretical and experimental values.

[b] References to each potential are given in brackets.

Thermal diffusion studies of the systems Ne-CO_2[30] and Ar-CO_2[31,32] have reported that α_T actually *increases* with *decreasing* temperature, which disagrees with the predictions of the Chapman Enskog theory. This apparent anomaly was investigated in this study for Ne-CO_2; the thermal conductivities of Ar and CO_2 are too similar for analysis with any degree of precision of Ar-CO_2 mixtures using the present apparatus.

The coefficients summarising the concentration dependence of $(\alpha_T)^{-1}$ at three temperatures are given in Table 7.13 and these show that α_T increases over the temperature range 270 to 324K by approximately 8 percent. Inspection of Table IV.8 (in Appendix IV) shows that this difference is approximately twice the sum of the maximum possible experimental errors at these temperatures.

This result does not support the conclusions of Weissman et al[30] who reported an increase in α_T with decreasing temperature.

Tests of spherical potentials for non spherical systems

The recent study[11] in this laboratory showed that the experimental thermal diffusion factors for mixtures of rare gases were almost all predicted within experimental error using the spherical potentials in the literature.

In this study transport properties have been measured for systems in which the 'true' potential is expected to be asymmetric and for which inelastic collisions may be important. The experimental results have been used to derive spherical potentials and to test the potential functions in the literature. Where the potentials have an asymmetric component this has been neglected in the calculation of transport properties. As the potentials derived as part of this study and taken from the literature are spherical they are only expected to approximate the 'true' asymmetric potentials.

The systems are considered in the order H_2- rare gases, D_2-rare gases, N_2-rare gases, CO_2-Ne and CH_4-rare gases. Also the difference between H_2-rare gas and D_2- rare gas interactions is investigated.

In Tables 7.22 to 7.27 the experimental D_{12}^0 and α_T values (smoothed at x_1=0.2 and x_1=0.8) are compared with values calculated using the potentials for unlike potential interactions in Table V.2 (Appendix V). The D_{12}^0 values have been used in these comparisons as at x_1=0 the diffusion coefficient is only a function of the unlike interaction.[38]

The quantum collision integrals of Taylor[34] have been used for hydrogen and deuterium.

Only the potentials for unlike interactions[35-41] best predicting the experimental D^{0}_{12} values in Table 7.22 were used to predict α_T values in Table 7.23; the predictions using the remaining potentials generally deviated from the experimental α_T values by greater than twice the maximum experimental error.

Inspection of Tables 7.22 and 7.23 shows that apart from some of the potentials obtained as part of this study, only the HFD potential of Andres et al[37] reproduces the experimental data adequately. This HFD potential was derived for D_2-Ne and only the spherical part of the asymmetric potential has been used.

The potentials for the rare gas-hydrogen systems have also been used to predict transport properties for the rare gas - deuterium systems; thus the potential functions which characterise all the interactions involving hydrogen are assumed to be exactly the same as those involving deuterium. Consequently any difference in the preoperties of corresponding systems is due entirely to the mass difference between hydrogen and deuterium.

Comparison of Tables 7.23 and 7.25 indicates that with exception of the HFD potential of Andres et al the difference between calculated and experimental values of α_T is greater for the deuterium systems.

To test the duality of the 'H_2' and 'D_2' potential the experimental data for the rare gas - hydrogen systems were corrected

Table 7.22[a,b,c]

Comparison of experimental and theoretical limiting diffusion coefficients, D^0_{12}, at 300K for the Rare Gas - Hydrogen Systems.

	Reference	$(D^0_{12})^{exp}$	$(D^0_{12})^{th}$	δ%
H_2-Ne				
LJ(12,6)	(35)	1.176	1.112	-5.4
LJ(15,6)	(36)		1.166	-0.8
HFD	(37)		1.171	-0.4
(10,6,8,γ=2.0)			1.176	0.0
H_2-Ar				
LJ(12,6)	(38)	0.824	0.771	-6.4
BC	(39)		0.799	-3.0
(12,6,8,γ=2.5)			0.824	0.0
H_2-Kr				
LJ(12,6) [13]	(40)	0.724	0.690	-4.7
LJ(12,6,8) [5]	(41)		0.671	-7.3
BC	(39)		0.708	-2.2
(11,6,8,γ=3.0)			0.724	0.0
H_2-Xe				
LJ(13,6) [13]	(40)	0.623	0.588	-5.6
LJ(12,6,8) [5]	(41)		0.596	-4.5
BC [14]	(39)		0.585	-6.1
HFD [17]	(38)		0.575	-8.3
(11,6,8,γ=3.0)			0.623	0.0

[a] The δ% are percentage differences between theoretical and experimental values.

[b] δ% values for the (m,6,8) potentials are zero because of the method used to obtain the potential parameters.

[c] (m,6,8) potentials obtained in this study.

Table 7.23[a,b,c]

Comparison between smoothed experimental and calculated α_T values for Rare Gas - Hydrogen Systems at 300K.

	x_1	$(\alpha_T)_{exp}$	δ% (m68)	δ% BC(39)	δ% HFD(37)
$Ne-H_2$	0.2	0.341	5.3		-0.3
	0.8	0.289	0.3		3.4
$Ar-H_2$	0.2	0.390	1.0	5.6	
	0.8	0.254	-1.6	2.0	
$Kr-H_2$	0.2	0.404	1.5		
	0.8	0.241	-0.4		
$Xe-H_2$	0.2	0.421	3.8		
	0.8	0.235	0.0		

a The numbers in parentheses are the references for the unlike potential functions.

b (m68) potentials obtained in this study.

c δ% are the percentage deviations between experimental and calculated values.

Table 7.24[a,b,c]

Comparison of experimental and theoretical limiting diffusion coefficients, D_{12}, at 300K for the Rare Gas - Deuterium Systems.

$(D^0_{12})_{exp}$	Potential	$(D^0_{12})_{th}$	$\delta\%$[a]	$(D^0_{12})_{corr.}$
		D_2-Ne		
0.871_3	HFD (37) (10,6,8,γ=2.0)	0.867_5 0.868_4	-0.4 -0.3	0.869_9
		D_2-Ar		
0.594_2	B-C (39) (12,6,8,γ=2.5)	0.578_6 0.596_3	-2.7 0.4	0.596_4
		D_2-Kr		
0.518_2	B-C (39) (11,6,8,γ=3.0)	0.506_2 0.515_8	-2.4 -0.5	0.516_1
		D_2-Xe		
0.446_5	B-C (39) (11,6,8,γ=3.0)	0.424_1 0.443_6	-5.3 -0.6	0.444_1

a The $\delta\%$ are percentage differences between theoretical and experimental values.

b The (m68) potentials are those obtained for corresponding hydrogen systems in this study.

c The numbers in parentheses after potentials are references.

Table 7.25[a,b]

Comparison between smoothed experimental and calculated α_T values for the Rare Gas - Deuterium Systems at 300K.

	x_1	$(\alpha_T)_{exp}$	$(\alpha_T)_{corr}$	δ% (m,6,8)	δ% HFD(37)	δ% B-C(39)
$Ne-D_2$	0.2	0.287	0.288	6.3	-0.4	-
	0.8	0.251	0.260	5.1	0.0	-
$Ar-D_2$	0.2	0.359	0.365	2.6	-	7.2
	0.8	0.238	0.246	1.8	-	5.1
$Kr-D_2$	0.2	0.386	0.392	3.2	-	5.3
	0.8	0.236	0.238	0.3	-	0.7
$Xe-D_2$	0.2	0.410	0.414	4.7	-	11.8
	0.8	0.231	0.233	1.1	-	5.8

a δ% is the percentage difference between calculated and experimental values.

b (m68) potentials obtained for corresponding hydrogen systems in this study.

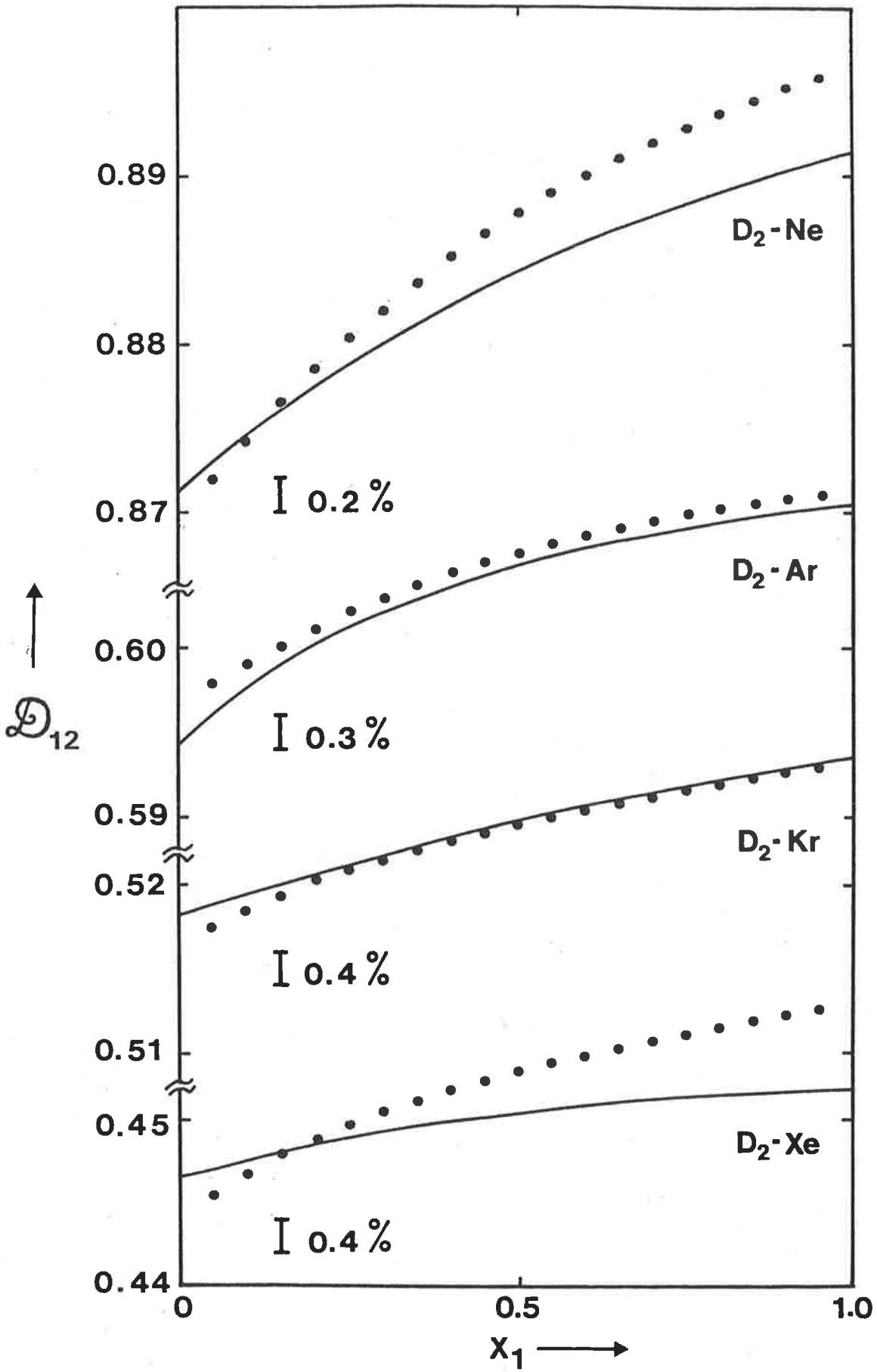

Figure 7.1 Graphs of D_{12} vs x_1 for Rare Gas - D_2 systems at 300K;

——— , smoothed experimental values;

• • • , smoothed values for Rare Gas - H_2 gas mixtures corrected to the reduced masses of the corresponding Rare Gas - D_2 systems.

to the reduced masses of the corresponding rare gas - deuterium systems using the Chapman Cowling expressions. The resulting values $(\overset{0}{D}_{12})_{corr}$ and $(\alpha_T)_{corr}$ are listed in Tables 7.24 and 7.25 and plotted for diffusion in Figure 7.1. The agreement between experimental and corrected values varies with system and mole fraction.

Experimental[42-48] and theoretical[49-51] evidence has already been reported to suggest that the potentials of H_2 and D_2 are slightly different; the second virial coefficient of D_2 is approximately 0.5cm^3 mol^{-1} less than that of H_2 at 300K.[42] Trengove and Dunlop[52] have measured the excess second virial coefficients, B^E,

$$B^E = B_{12}-(B_{11}+ B_{22})/2 \qquad (7.7)$$

where B_{11} and B_{22} are coefficients for like interactions and B_{12} the coefficients for the unlike interaction, for Ar-H_2 and Ar-D_2 at 300K. The results indicate the $B_{Ar\text{-}H_2}$ and $B_{Ar\text{-}D_2}$ values are identical.

Inspection of Table 7.26 shows that except for the SPFD potential of Keil et al[53] for He-N_2 the difference between theory and experiment is much larger than experimental error, especially for the systems Ne-N_2 and Ar-N_2. The SPFD potential predicted limiting binary diffusion coefficients that agree with literature values[6] to approximately 1.5%. The potentials of Tully and Lee[54] for Ar-N_2 and Kr-N_2 predicted D_{12}° values, which differed from experimental results by as much as 15%.

From the results of their differential scattering cross section measurements Keil et al concluded that for He-N_2 the spherical average of the anisotropic potential obtained using their data was indistinguishable from the SPFD potential obtained by a central field analysis.

Wood and Curtiss[55] have shown that the asymmetry of the Ar-N_2 potential and the presence of inelastic collisions are important when calculating thermal diffusion factors. Using the LJ(12,6) potential to model both the spherical and asymmetric parts of the Ar-N_2 interaction they found that at $x_1 = 0.86$ the value of α_T at 300K was 29.7% *lower* when only the spherical portion of the total potential was employed. If one can assume that approximately the same correction applies for similar potential forms then the differences for Ar-N_2 shown in Table 7.26 would almost disappear.

In a study of rotational relaxation times of four rare gas - nitrogen systems Kistemaker and de Vries[56] found that Ne-N_2 and Ar-N_2 showed much smaller rotational collision numbers than

$He-N_2$ and $Xe-N_2$. Thus $Ne-N_2$ and $Ar-N_2$ are expected to have a greater collisional efficiency for translational-rotational energy transfer, and these systems show the greatest deviations in Table 7.26.

In addition the calculations of Kelley and Wolfsberg[57] and Gelb and Kapral[58] indicate that for homonuclear diatomic-atomic systems optimal rotational energy transfer occurs when the atomic and molecular masses are approximately equal.

Table 7.26[a,b,c]

Comparison between smoothed experimental and calculated α_T values for the Rare Gas - Nitrogen Systems at 300K.

	x_1	$(\alpha_T)_{exp}$	δ% (m68)	δ% SPFD	δ% LJ(12,6)	δ% LJ(20,6)
$He-N_2$	0.2	0.502	10.8(6)	1.6(53)		
	0.8	0.293	10.2	2.0		
$Ne-N_2$	0.2	0.079_6	72.4			
	0.8	0.058_6	82.3			
$Ar-N_2$	0.2	0.075_1	-24.5(6)		-32.3(54)	1.8(54)
	0.8	0.077_7	-25.3		-38.5	-15.9
$Kr-N_2$	0.2	0.146	-1.6		-13.2(54)	38.1(54)
	0.8	0.131	-7.8		-22.9	18.4
$Xe-N_2$	0.2	0.174	4.0			
	0.8	0.137	-4.7			

a δ% is the percentage difference between calculated and experimental values.

b The numbers in parentheses are references.

c (m68) potentials for $Ne-N_2$, $Kr-N_2$ and $Xe-N_2$ obtained in this study.

Using the (m68) potential of Robjohns and Dunlop[59] with the relevant potentials from Table V.1 α_T values have been calculated at 300K for comparison with the experimental Ne-CO_2 data. At x_1 = 0.8 the calculated values were approximately 30 percent higher than the experimental data.

Inspection of Table 7.27 shows that apart from the (m68) potentials[8] for Ar-CH_4, Kr-CH_4 and Xe-CH_4 no potential predicts both the experimental α_T and D_{12}^0 values within experimental error.

Kistemaker et al[66,67] measured rotational relaxation times for four rare gas - CH_4 systems and found that He-CH_4 and Ne-CH_4 have much smaller rotational collision numbers than Ar-CH_4 and Xe-CH_4. Thus the two former systems are expected to have a greater collisional efficiency for translational-rotational energy transfer.

Table 7.27[a]

Comparison of smoothed experimental and calculated values of α_T at 300K for Rare Gas - Methane Systems.

	Potential	Reference	$\delta\%(\alpha_T)$ $(x_1=0.2)$	$\delta\%(\alpha_T)$ $(x_1=0.8)$	$\delta\%(D_{12}^0)$
He-CH_4	(10,6,8,γ=2.0)	(8)	17.2	16.2	0.1
	LJ(12,6)	(61)	5.9	15.0	19.3
	SPFD	(60)	18.9	16.3	-3.0
Ne-CH_4	(20,6,8,γ=0)	(8)	-136.4[b]	-51.9	0.2
Ar-CH_4	(20,6,8,γ=0)	(8)	-0.6	0.6	0.1
	MSMSV	(62)	-3.8	-5.9	-3.6
	MSV	(63)	-3.8	-2.0	2.0
	LJ(12,6)	(64)	0.0	-2.6	-3.8
	LJ(18,6)	(65)	13.8	10.2	-5.6
Kr-CH_4	(11,6,8,γ=0.25)	(8)	0.5	-2.7	-0.1
Xe-CH_4	(13,6,8,γ=2.0)	(8)	3.7	-1.2	+0.1

[a] The δ values are the deviations between calculated and experimental data - the experimental D_{12}^0 values are those of Trengove, Robjohns and Dunlop.[8]

[b] The predicted value of α_T is negative at $x_1 = 0.2$

Comparison with data in literature

The smoothed experimental thermal diffusion factors measured in this study are compared with results selected from the literature in Tables 7.28 to 7.31 and Figure 7.2.

Several workers have reported results with maxima or minima in the concentration dependence of α_T, and these results have usually been interpreted in terms of the presence of inelastic collisions.

Schaschkov, Zogothyhena and Abramenko[75] have reported a very large minimum for Ar-N_2 at 326K, whilst the results of this study at 300K show no such behaviour.

Batabyal and Barua[76] have measured the concentration dependence of α_T for Ne-CO_2 at 343K and the data in Table 7.13 has been used to correct the original data to the temperatures for display in Table 7.31.

Minima in the composition dependence of the thermal diffusion factors have been reported by several workers for Ar-CH_4. The results of this study at 300K are compared with those of Heintz et al[77] at 306K and the minimum of Acharyya and Barua[78] at 351K in Figure 7.2. Shahin et al[79] have also reported minima at much higher temperatures. However, the results in this study are perfectly consistent with those of Stevens and De Vries.[80]

Table 7.28

Comparison of present α_T values with results selected from the literature for Ar-Kr.

x_1	This study	Literature	Reference
		$\bar{T}$=255.3K	
0.5	0.068_5	0.056_8	(68)
		0.054_4	(69)
0.03	0.077	0.036	(70)
trace Kr	0.077	0.08	(71)
		$\bar{T}$=300K	
0.03	0.103	0.066	(70)
trace Kr	0.104	0.12	(71)

Table 7.29

Comparison of present α_T values at 300K with results selected from the literature for $Kr-D_2$ and $Xe-D_2$.

	x_1	This study	Literature	Reference
$Xe-D_2$	trace Xe	0.543	0.58_3	(72)
$Kr-D_2$	trace Kr	0.491	0.46_4	(73)
$Kr-D_2$	trace D_2	0.209	0.19_2	(73)

Table 7.30

Comparison of present α_T values at 300K with results selected from the literature for $Ar-N_2$, $Kr-N_2$ and $Xe-N_2$.

	x_1	This study	Literature	Reference
$Ar-N_2$	0.51	0.0764	0.07_7	(74)
$Kr-N_2$	0.01	0.152	0.09_5	(73)
$Kr-N_2$	0.31	0.143	0.08_4	(74)
$Xe-N_2$	trace Xe	0.191	0.21_7	(72)

Table 7.31[a]

Comparison of present α_T values at 300K with results selected from the literature for Ne-CO_2.

	Trace CO_2		
	270K	300K	324K
Present results	0.23_6	0.24_6	0.25_2
Weissman et al (30)	0.29_0	0.27_7	0.26_9
Batabyal and Barua (76)	0.31_5	0.32_6	0.33_5

[a] The results of Batabyal and Barua have been corrected to the above temperatures using the data in Table 7.13.

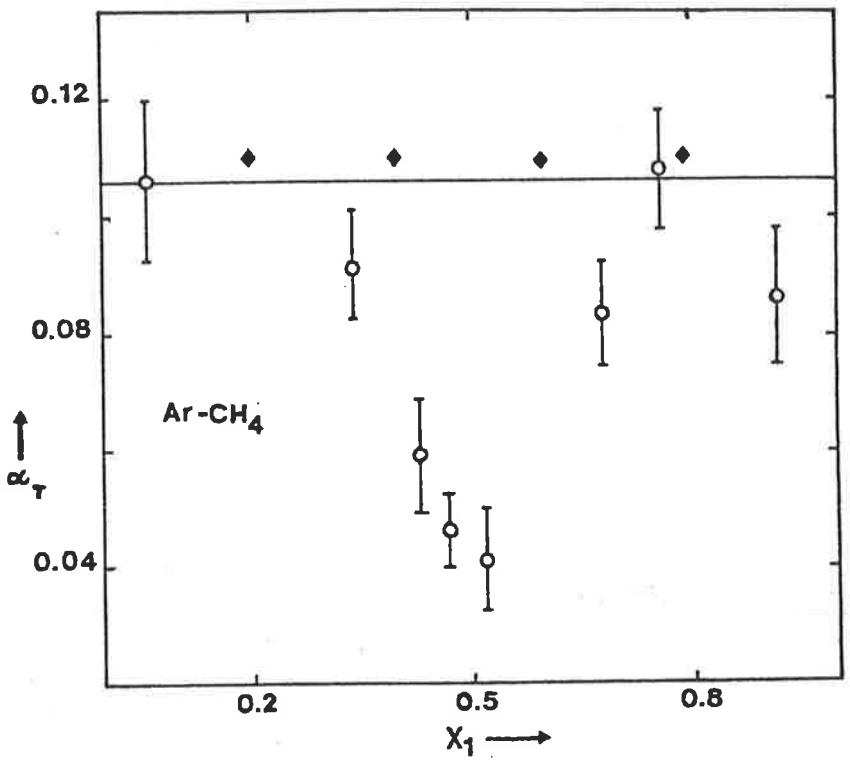

Figure 7.2 Graph of α_T vs x_1 for Ar-CH_4;

—— , smoothed experimental values at 300K (this work);

◆ , Heintz et. al. at 306K (77);

o , Acharyya and Barua at 351K (78).

The preceeding discussion shows that, in general, systems containing a rare gas and either a diatomic or polyatomic are not adequately described by spherical potentials when inelastic collisions are neglected. The results of Wood and Curtiss[56] for Ar-N_2 show that neglecting the asymmetry of the system can lead to rather large discrepancies. Until similar calculations have been performed for other systems the effect of the anisotropic portion of the potential can only be speculative. The studies of Kistemaker et al[56,66,67] indicate that the trends observed in discrepancies between calculated and experimental α_T values in this work may be due in part to the existence of inelastic collisions. This is further supported by the calculations of Kelly and Wolfsberg[57] and Gelb and Kapral.[58]

A study of thermal diffusion in mixtures of SF_6 with the rare gases is currently underway in this laboratory.[81] The results for He-SF_6 and Ne-SF_6 show excellent agreement with the values predicted using the asymmetric potentials of Pack and coworkers[82,83] in the limit as $x_1 \rightarrow 0$. The collision integrals for the rare-gas interactions were computed by Pack[84] using the infinite order sudden approximation (105A)[85-87] to obtain cross-sections and then the Monchick-Mason[88] approximation to derive the omega integrals. The SF_6 collision integrals were calculated using a crude estimate of the potential obtained in this laboratory.[89] A better potential for SF_6 is expected to reduce the deviation as $x_1 \rightarrow 1$.

REFERENCES

1. I. Amdur and T.F. Schatzki, *J.Chem.Phys.* 29 1 (1958).
2. T.R. Marrero and E.A. Mason, *J.Phys.Chem. Ref. Data* 1 3 (1972).
3. M.A. Yabsley, P.J. Carson and P.J. Dunlop, *J.Phys.Chem.* 77 703 (1973).
4. S. Chapman and T.G. Cowling, *Mathematical Theory of Non-Uniform Gases*, 3rd edition, Cambridge University Press (1970).
5. E.A. Mason, *J.Chem.Phys.* 27 75 (1957).
6. P.S. Arora, H.L. Robjohns, I.R. Shankland and P.J. Dunlop, *Chem.Phys.Lett.* 59 478 (1978).
7. P.S. Arora, H.L. Robjohns, T.N. Bell and P.J. Dunlop, *Aust.J.Chem.* 33 1993 (1980).
8. R.D. Trengove, H.L. Robjohns and P.J. Dunlop, *Ber. Bunsenges.Phys.Chem.* 86 951 (1982).
9. P.S. Arora, H.L. Robjohns and P.J. Dunlop, *Physica* 95A 561 (1979).
10. M.F. Laranjeira, *Physica* 26 409, 417 (1970).
11. R.D. Trengove, H.L. Robjohns, T.N. Bell, M.L. Martin and P.J. Dunlop, *Physica* 108A 488 (1981).
12. J.Brewer, *Determination of Mixed Virial Coefficients*, Report No. MRL-2915-C, Airforce office of Scientific Research, No 67-2795 (1967).
13. J.H. Dymond and E.B. Smith, *The Virial Coefficients of Pure Gases and Mixtures*, Oxford University Press, Oxford (1980).

14. M.L. Martin, R.D. Trengove, K.R. Harris and P.J. Dunlop, *Aust.J.Chem.* 35 1525 (1982).

15. R.A. Aziz, V.P.S. Nain, J.S. Carley, W.L. Taylor and G.T. McConville, *J.Chem.Phys.* 70 4430 (1979).

16. R.A. Aziz, *High Temp.-High Press.* 12 565 (1980).

17. R.A. Aziz and H.H. Chen, *J.Chem.Phys.* 67 5719 (1977).

18. J.A. Barker, R.O. Watts, J.K. Lee, T.P. Schafer and Y.T. Lee, *J.Chem.Phys.* 61 3081 (1974).

19. E.A. Mason and E.W. Rice, *J.Chem.Phys.* 22 522 (1954).

20. P.S. Arora, *Ph.D. Thesis*, University of Adelaide (1979).

21. J.F. Ely and H.J.M. Hanley, *Molec.Phys.* 30 565 (1975).

22. G.P. Matthews and E.B. Smith, *Molec.Phys.* 32 1719 (1976).

23. R. Ahlrichs, R. Penco and G. Scoles, *Chem.Phys.* 19 119 (1977).

24. R.A. Aziz, P.N. Riley, U. Buck, G. Mancke, J. Schleusener, G. Scoles and U.Valbusa, *J.Chem.Phys.* 71 2637 (1979).

25. R.A. Aziz and A. van Dalen, *J.Chem.Phys.* 78 2413 (1983).

26. P.S. Arora, H.L. Robjohns and P.J. Dunlop, *Physica* 95A 561 (1979).

27. R.A. Aziz, J. Presley, U. Buck and J. Schleusener, *J.Chem.Phys.* 70 4737 (1979).

28. U. Buck, F. Huisken, H. Pauly and J. Schleusener, *J.Chem.Phys.* 68 3334 (1978).

29. G.C. Maitland and W.A. Wakeham, *Mol.Phys.* 35 1443 (1978).

30. S. Weissman, S.C. Saxena and E.A. Mason, *Phys.Fluids* 4 643 (1961).

31. L. Waldman, *Z.Naturforsch.* 4a 105 (1949).

32. J.R. Cozens and K.E. Grew, *Phys.Fluids* 7 1395 (1964).

33. K.R. Harris, T.N. Bell and P.J. Dunlop, *Canad.J.Phys.* 50 1644 (1972).

34. W.L. Taylor, *J.Chem.Phys.* 57 832 (1972).

35. R.W. Bickes, G. Scoles and K.M. Smith, *Canad.J.Phys.* 53 435 (1975).

36. A.L. Dunker and R.G. Gordon, *J.Chem.Phys.* 68 700 (1978).

37. J. Andres, U. Buck, F. Huisken, J. Schleusener and F. Torello, *J.Chem.Phys.* 73 5620 (1980).

38. A.M. Rulis, K.M. Smith and G. Scoles, *Canad.J.Phys.* 56 753 (1978).

39. R.J. LeRoy, J. Carley and J.E. Grabenstetter, *Faraday Discuss.Chem.Soc.* 62 169,303 (1977).

40. R.J. LeRoy and J. Van Kranendonk, *J.Chem.Phys.* 61 4750 (1974).

41. J.P. Toennies, W. Welz and G. Wolf. *J.Chem.Phys.* 71 614 (1979).

42. A. Michels, W. de Graaff and C.A. ten Seldam, *Physica* 26 393 (1960).

43. H.F.P. Knaap, L.J.F. Hermans, R.M. Jonkman and J.J.M. Beenakker, *Faraday Discuss.Chem.Soc.* 40 135 (1965).

44. I. Ahmur and J.W. Beatty, *J.Chem.Phys.* 42 3361 (1965).

45. E.A. Mason, B.K. Annis and M. Islam, *J.Chem.Phys.* 42 3364 (1965).

46. E.A. Mason, I. Ahmur and I. Oppenheim, *J.Chem.Phys.* 43 4458 (1965).

47. J.M.J. Coremans, A. van Itterbeck, J.J.M. Beenakker, J.F.P. Knaap and P. Zandbergen, *Physica* 24 557 (1958); 24 1102 (1965).

48. J. Kestin, S.T. Ro and W.A. Wakeham, *J.Chem.Soc. Faraday Trans.I* 68 2316 (1972).

49. E. Ishiguro, T. Arai, M. Mizushima and M. Kotani, *Proc. Phys.Soc.* 65 178 (1952).

50. J. de Boer, *Physica* 9 363 (1942); 10 357 (1943)

51. K.F.P. Knaap and J.J.M. Beenakker, *Physica* 27 523 (1961).

52. R.D. Trengove and P.J. Dunlop, *Ber.Bunsenges.Phys.Chem.* 86 628 (1982).

53. M. Keil, J.T. Slankas and A. Kuppermann, *J.Chem.Phys.* 70 541 (1979).

54. F.P. Tully and Y.L. Lee, *J.Chem.Phys.* 57 866 (1972).

55. R.R. Wood and C.F. Curtiss, *J.Chem.Phys.* 70 5792, 5798 (1979).

56. P.G. Kistemaker and A.E. de Vries, *Chem.Phys.* 7 371 (1975).

57. J.D. Kelley and M. Wolfsberg, *J.Chem.Phys.* 53 2967 (1970).

58. A. Gelb and R. Kapral, *Chem.Phys.Lett.* 17 397 (1972).

59. H.L. Robjohns and P.J. Dunlop, *Ber.Bunsenges.Phys.Chem.* 85 655 (1981).

60. J.T. Slankas, M. Keil and A. Kuppermann, *J.Chem.Phys.* 70 1482 (1979).

61. H.P. Butz, R. Feltgen, H. Pauly and H. Vehmeyer, *Z.Phys.* 247 70 (1971).

62. U. Buck, T. Schleusener, D.J. Malik and D. Secrest, *J.Chem.Phys.* 74 1707 (1981).

63. R. Behrens, A. Freedman, R.R. Herm and T.P. Parr, *Chem.Phys.Lett.* 36 446 (1976).

64. J. Bellm, W. Reineke, K. Schäfer and B. Schramm, *Ber.Bunsenges.Phys.Chem.* 78 282 (1974).

65. R. Hahn, K. Schäfer and B. Schramm, *Ber.Bunsenges.Phys. Chem.* 78 287 (1974).

66. P.G. Kistemaker, M.M. Hanna, A. Tom and A.E. de Vries, *Physica* 60 459 (1972).

67. P.G. Kistemaker, M.M. Hanna and A.E. de Vries, *Physica* 78 457 (1974).

68. K.E. Grew and J.N. Mundy, *Phys.Fluids* 4 1325 (1961).

69. W.L. Taylor, *J.Chem.Phys.* 72 4973 (1980).

70. K.E. Grew and W.A. Wakeham, *Mol.Phys.* 4 1548 (1971).

71. A.E. Humphreys and E.A. Mason, *Phys.Fluids* 13 65 (1970).

72. D. Heymann and J. Kistemaker, *Physica* 25 556 (1959).

73. E.A. Mason, M. Islam and S. Weissman, *Phys.Fluids* 7 1011 (1964).

74. K.E. Grew, F.A. Johnson and N.E.J. Neal, *Proc.Roy.Soc.* A224 513 (1954).

75. A.G. Schaschkov, A.F. Zogothyhena and T.N. Abramenko, *Inzh.Fiz.Zh.* 24 1045 (1973).

76. A.K. Batabyal and A.K. Barua, *J.Chem.Phys.* 48 2557 (1968).

77. A. Heintz, R.N. Lichtenthaler and K. Schäfer, *Ber.Bunsenges. Phys.Chem.* 79 426 (1975).

78. S. Acharyya and A.K. Barua, *J.Phys.Soc.Japan* 31 250 (1971).

79. F. Shahin, B.T. Abel-Latif and N. Farag, *J.Chem.Phys.* 73 1465 (1980).

80. G.A. Stevens and A.E. De Vries, *Physica* 39 346 (1968).

81. R.D. Trengove, H.L. Robjohns and P.J. Dunlop, *(to be published)*.

82. R.T. Pack, J.J. Valentin and J.B. Cross, *J.Chem.Phys.* 77 5486 (1982).

83. R.T. Pack, E. Piper, G.A. Pfeffer and J.P. Toennies, *J.Chem.Phys.* in press.

84. R.T. Pack, *Private Communication*.

85. T.P. Tsien and R.T. Pack, *Chem.Phys.Lett.* 5 54 (1970); 8 579 (1971).

86. R.T. Pack, *J.Chem.Phys.* 60 633 (1974).

87. G.A. Parker, and R.T. Pack, *J.Chem.Phys.* 68 1585 (1978).

88. L. Monchick and E.A. Mason, *J.Chem.Phys.* 35 1676 (1961).

89. R.D. Trengove, H.L. Robjohns, M.L. Martin and P.J. Dunlop, *Physica* 108A 502 (1981).

APPENDIX I

Approximations for Transport Properties using the Chapman-Enskog Theory.

The supplementary formula to section (2.2) needed to calculate the diffusion coefficient to the second approximation and the thermal diffusion factor to the first approximation are given here.

Diffusion: Chapman-Cowling scheme

$$f_D^{(2)} = 1/(1-\Delta_{12}) \tag{I.1}$$

with $$\Delta = \frac{1}{10}(6C_{12}^{*}-5)^2 \frac{x_1^2P_1 + x_2^2P_2 + x_1x_2P_{12}}{x_1^2Q_1 + x_2^2Q_2 + x_1x_2Q_{12}} \tag{I.2}$$

$$P_1 = \frac{2M_1^2}{M_2(M_1+M_2)} \left(\frac{2M_2}{M_1+M_2}\right)^{\frac{1}{2}} \left(\frac{\Omega_{11}(2,2)^{*}}{\Omega_{12}(1,1)^{*}}\right) \left(\frac{\sigma_{11}}{\sigma_{12}}\right)^2 \tag{I.3}$$

$$P_{12} = 15\left(\frac{M_1-M_2}{M_1+M_2}\right)^2 + \frac{8M_1M_2A_{12}^{*}}{(M_1+M_2)} \tag{I.4}$$

$$Q_1 = \frac{2}{M_2(M_1+M_2)} \left(\frac{2M_2}{M_1+M_2}\right)^{\frac{1}{2}} \left(\frac{\Omega_{11}(2,2)^{*}}{\Omega_{12}(1,1)^{*}}\right) \left(\frac{\sigma_{11}}{\sigma_{12}}\right)^2$$

$$X\left[\left(\frac{5}{2} - \frac{6}{5}B_{12}^{*}\right) M_1^2 + 3M_2^2 + \frac{8}{5}M_1M_1A_{12}^{*}\right] \tag{I.5}$$

$$Q_{12} = 15\left(\frac{M_1-M_2}{M_1+M_2}\right)^2\left(\frac{5}{2} - \frac{6}{5}B_{12}^*\right) + \frac{4M_1M_2A_{12}^*}{(M_1+M_2)^2}\left(11 - \frac{12}{5}B_{12}^*\right)$$

$$+ \frac{8(M_1+M_2)}{5(M_1M_2)^{\frac{1}{2}}}\left[\frac{\Omega_{11}^{(2,2)*}}{\Omega_{12}^{(1,1)*}}\right]\left[\frac{\Omega_{22}^{(2,2)*}}{\Omega_{12}^{(1,1)*}}\right]\left(\frac{\sigma_{11}}{\sigma_{12}}\right)^2\left(\frac{\sigma_{22}}{\sigma_{12}}\right)^2. \quad \text{(I.6)}$$

The functions A_{12}^*, B_{12}^* and C_{12}^* are ratios of collision integrals and are given below; M_1 and M_2 are the molecular weights of species 1 and 2 respectively, and the remaining variables are defined in chapter 2. The relations for P_2 and Q_2 are obtained from those for P_1 and Q_1 by an interchange of subscripts.

$$\left.\begin{aligned} A_{12}^* &= \Omega_{12}^{(2,2)*} / \Omega_{12}^{(1,1)*} \\ B_{12}^* &= \{5\Omega_{12}^{(1,2)*} - 4\Omega_{12}^{(1,3)*}\} / \Omega_{12}^{(1,1)*} \\ C_{12}^* &= \Omega_{12}^{(1,2)*} / \Omega_{12}^{(1,1)*} \end{aligned}\right\} \quad \text{(I.7)}$$

Diffusion: Kihara scheme

$$g_D^{(2)} = 1 + \Delta' \quad \text{(I.8)}$$

where Δ' is of exactly the same form as equation (I.2) but with differing expressions for the Q's:

$$Q_1' = \frac{2}{M_2(M_1+M_2)}\left(\frac{2M_2}{M_1+M_2}\right)^{\frac{1}{2}}\left[\frac{\Omega_{11}^{(2,2)*}}{\Omega_{12}^{(1,1)*}}\right]\left(\frac{\sigma_{11}}{\sigma_{12}}\right)^2$$

$$X\left[M_1^2 + 3M_2^2 + \frac{8}{5}M_1M_2A_{12}^*\right] \qquad \text{(I.9)}$$

$$Q_{12}' = 15\left(\frac{M_1-M_2}{M_1+M_2}\right)^2 + \frac{32M_1M_2A_{12}^*}{(M_1+M_2)^2} + \frac{8(M_1+M_2)}{5(M_1M_2)^{\frac{1}{2}}}$$

$$X\left[\frac{\Omega_{11}^{(2,2)*}}{\Omega_{12}^{(1,1)*}}\right]\left[\frac{\Omega_{22}^{(2,2)*}}{\Omega_{12}^{(1,1)*}}\right]\left(\frac{\sigma_{11}}{\sigma_{12}}\right)^2\left(\frac{\sigma_{22}}{\sigma_{12}}\right)^2 \quad . \qquad \text{(I.10)}$$

The expression for Q_2' is obtained from that for Q_1' by the interchange of subscripts.

Thermal Diffusion

The first approximation for the thermal diffusion factor, for both approximation schemes, has the form

$$[\alpha_T]_1 = (6C_{12}^*-5)\frac{x_1S_1 - x_2S_2}{x_1^2Q_1 + x_2^2Q_2 + x_1x_2Q_{12}} \qquad \text{(I.11)}$$

where

$$S_1 = \frac{M_1}{M_2}\left(\frac{2M_2}{M_1+M_2}\right)^{\frac{1}{2}}\left[\frac{\Omega_{11}^{(2,2)*}}{\Omega_{12}^{(1,1)*}}\right]\left(\frac{\sigma_{11}}{\sigma_{12}}\right)^2$$

$$- \frac{4M_1M_2A_{12}^*}{(M_1+M_2)^2} - \frac{15M_2(M_2-M_1)}{2(M_1+M_2)^2} \quad . \qquad \text{(I.12)}$$

The expression for S_2 is obtained from that for S_1 by interchange of subscripts, but the expressions for the Q's differs for the two schemes, with those for the Chapman-Cowling scheme given by equations (I.5) and (I.6) and those for the Kihara scheme given by equations (I.9) and (I.10).

APPENDIX II

Concentration and Temperature Dependence of α_T

The thermal diffusion factor, α_T, is expanded in a Taylor series about the point $(\bar{x}_1, \bar{T})$ and this is then inserted in the basic differential equation for thermal diffusion[1,2] to be integrated between the limits (x_1, T) for the cold bulb and (x_1', T') for the hot bulb of the cell. That is

$$\alpha_T = \alpha^0 + D_1(x_1-\bar{x}_1) + D_2(T-\bar{T}) + \ldots \qquad \text{(II.1)}$$

$$= \alpha^0[1 + R_1(x_1-\bar{x}_1) + R_2(T-\bar{T}) + \ldots] \qquad \text{(II.2)}$$

with $$R_1 = \frac{1}{\alpha^0}\left(\frac{\partial\alpha_T}{\partial x_1}\right)_{\bar{x}_1,\bar{T}}$$

$$R_2 = \frac{1}{\alpha^0}\left(\frac{\partial\alpha_T}{\partial T}\right)_{\bar{x}_1,\bar{T}} \qquad \text{(II.3)}$$

$$\alpha^0 = \alpha_T(\bar{x}_1, \bar{T})$$

The basic differential equation for thermal diffusion

$$\frac{dx_1}{dz} = -\alpha_T(1-x_1)x_1\frac{d\ln T}{dz} \qquad \text{(II.4)}$$

can be rewritten in terms of equations (II.1) to (II.3) as

$$dx_1 = -\alpha^0(1 + R_1(x_1-\bar{x}_1) + R_2(T-\bar{T})(1-x_1)x_1 d\ln T \qquad \text{(II.5)}$$

At this stage to avoid unnecessary complexity the expansions in terms of $\bar{x}_1$ and $\bar{T}$ are considered individually. Thus equation (II.5) is simplified for the expansion about $\bar{x}_1$ to

$$dx_1 = -\alpha^0(1 + R_1(x_1-\bar{x}_1))(1-x_1)x_1 d\ln T \qquad \text{(II.6)}$$

which may be written as

$$dx_1\left(\frac{a}{x_1} + \frac{b}{1-x_1} + \frac{c}{1+R_1(x_1-\bar{x}_1)}\right) = -\alpha^0 d\ln T \qquad \text{(II.7)}$$

where $a = 1/(1-R_1\bar{x}_1)$

$b = 1/(1+R_1(1-\bar{x}_1))$ (II.8)

$c = -(R_1)^2ab$

Equation (II.8) is then integrated between the limits (x_1, T) for the cold bulb and (x_1', T') for the hot bulb of the cell to give

$$a\ln(x_1/x_1') + b\ln((1-x_1')/(1-x_1)) + (c/R_1)\ln((1 + aR_1x_1)/(1 + aR_1x_1')) = \alpha^0\ln(T'/T) \quad \text{(II.9)}$$

Equation (II.9) is then written in terms of the experimental thermal diffusion factor to give

$$\alpha^0 = \alpha_T^{exp} + A\ln(x_1/x_1') + B\ln[(1-x_1)/(1-x_1')] + C\ln[(1 + aR_1x_1)/(1 + aR_1x_1')] \quad \text{(II.10)}$$

where $$\alpha_T^{exp} = \ln[(x_1/x_1')((1-x_1')/(1-x_1)]/\ln(T'/T). \quad \text{(II.11)}$$

$A = aR_1\bar{x}_1$

$B = bR_1(1-\bar{x}_1)$ (II.12)

$C = c/R_1 = -abR_1$

Using the same procedure for the expansion about $\bar{T}$ equation (II.5) is simplified to

$$dx_1 = -\alpha^0(1 + R_2(\bar{T}-T))x_1(1-x_1)d\ln T \quad \text{(II.13)}$$

which is written in the useful form

$$\frac{dx_1}{x_1(1-x_1)} = -\alpha^0(1 + R_2(\bar{T}-T))d\ln T \quad \text{(II.14)}$$

and integration between the limits (x_1, T) and (x_1', T') for the cold and hot bulbs of the cell respectively gives the following result

$$\ln((x_1/x_1')(1-x_1')/(1-x_1)) = \alpha^0[\ln(T'/T) + R_2\Delta T - R_2\bar{T}\ln(T'/T)] \quad . \quad \text{(II.15)}$$

Equation (II.15) can then be written in terms of the experimental thermal diffusion factor, α_T^{exp}, to give

$$\alpha^0 = \alpha_T^{exp} + \alpha^0 R_2(\bar{T}-(T'-T)/\ln(T'/T)) \quad . \qquad (II.16)$$

Thus equations (II.11) and (II.16) can be combined as

$$\alpha_T(\bar{x}_1, \bar{T}) = \alpha_T^{exp} + \Delta_1 + \Delta_2$$

where the terms Δ_1 and Δ_2 are defined in equations (II.10) and (II.16) respectively.

REFERENCES

1. E.A. Mason, R.J. Munn, and F.J. Smith, *Advances in Atomic and Molecular Physics*, Vol.2, p. 37, Academic Press (1966).

2. G.C. Maitland, M. Rigby, E.B. Smith, and W.A. Wakeham, *Intermolecular Forces*, p. 354, Oxford University Press (1981).

APPENDIX III

Two Bulb Diffusion Data

The data summarised in sections 7.2 and 7.3 are presented in the following tables.

The symbols are defined below.

x_1 : Mole fraction of the heavy component calculated from partial pressures.

P : Pressure at which the experiment was performed (Torr).

T : Temperature (K)

D_{12}: Mutual Diffusion Coefficient ($cm.^2 s^{-1}$).

Table III.1

Insert used in measurement of D_{12}

System	Internal Diameter of Insert Used (cm)
Ne-H_2	0.16
Ar-H_2	0.16
Kr-H_2	0.16
Xe-H_2	0.16
Ne-D_2	0.16
Ar-D_2	0.16
Kr-D_2	0.16
Xe-D_2	0.25
Ne-N_2	0.25
Kr-N_2	0.25
Xe-N_2	0.25

Table III.2

Concentration Dependence of D_{12} for Ne-H_2 at 300K

Expt. #	x_1	P	T	D_{12}
1267	0.100_3	108.5	299.98	1.184
1258	0.101_7	108.6	299.98	1.183
1268	0.125_6	108.6	299.98	1.187
1269	0.126_8	108.5	299.98	1.187
1266	0.150_9	108.6	299.98	1.187
1256	0.152_4	108.7	299.98	1.188
1260	0.201_2	108.7	299.98	1.192
1262	0.302_5	108.9	299.98	1.197
1264	0.403_0	109.1	299.98	1.202
1263	0.454_2	139.0	299.98	1.204
1265	0.551_6	145.1	299.98	1.209
1259	0.897_8	108.7	299.98	1.218
1257	0.898_6	108.6	299.98	1.218

Table III.3

Temperature Dependence of D_{12} for Ne-H_2.

Expt. #	x_1	P	T	D_{12}
1390	0.124_9	135.0	278.00	1.042
1392	0.125_2	135.0	278.00	1.041
1395	0.125_1	135.0	281.21	1.064
1396	0.125_2	135.0	281.21	1.063
1398	0.125_5	135.0	285.26	1.089
1399	0.125_7	135.0	285.26	1.089
1400	0.124_7	143.1	289.14	1.114
1401	0.124_6	143.0	289.14	1.115
1403	0.198_9	143.5	292.78	1.142
1404	0.200_8	143.2	292.78	1.143
1408	0.157_2	147.5	296.04	1.162
1409	0.157_2	147.5	296.04	1.163
1350	0.300_1	150.4	308.15	1.225
1351	0.299_6	150.5	308.15	1.226
1352	0.300_4	150.5	312.18	1.279
1353	0.299_6	150.6	312.18	1.278
1354	0.300_3	150.7	316.26	1.309
1355	0.301_1	150.6	316.26	1.308
1357	0.301_5	150.8	320.30	1.336
1358	0.302_3	150.9	320.30	1.336
1359	0.301_3	173.9	323.15	1.356
1360	0.301_5	173.9	323.15	1.358

Table III.4

Concentration Dependence of D_{12} for Ar-H_2 at 300K

Expt. #	x_1	P	T	D_{12}
1230	0.050_8	108.5	299.98	0.8260
1231	0.064_7	108.9	299.98	0.8270
1225	0.100_7	108.9	299.98	0.8281
1221	0.156_9	109.1	299.98	0.8295
1220	0.201_5	109.4	299.98	0.8310
1227	0.408_5	110.2	299.98	0.8365
1229	0.506_6	109.7	299.98	0.8375
1226	0.507_0	111.0	299.98	0.8380
1228	0.592_1	110.1	299.98	0.8395
1223	0.896_4	108.8	299.98	0.8430
1224	0.953_9	108.8	299.98	0.8435

Table III.5

Temperature Dependence of D_{12} for Ar-H_2

Expt.#	x_1	P	T	D_{12}
1282	0.147_4	108.2	277.76	0.7251
1283	0.149_0	108.3	277.76	0.7246
1284	0.146_7	108.4	277.76	0.7239
1285	0.150_0	108.4	281.32	0.7418
1286	0.150_0	108.6	281.32	0.7418
1288	0.149_9	108.5	285.20	0.7588
1290	0.148_8	108.5	288.87	0.7753
1291	0.150_5	108.7	293.22	0.7959
1292	0.150_0	108.7	293.22	0.7955
1295	0.149_5	108.7	301.48	0.8350
1296	0.148_4	108.7	301.48	0.8358
1297	0.151_6	108.7	305.19	0.8540
1298	0.149_6	108.7	305.19	0.8543
1299	0.200_0	108.8	309.16	0.8758
1300	0.248_8	108.8	309.16	0.8781
1303	0.202_0	108.7	313.48	0.8971
1304	0.250_5	108.8	318.15	0.9220
1305	0.249_1	108.8	318.15	0.9228
1306	0.250_4	108.8	318.15	0.9220
1308	0.252_0	108.8	323.03	0.9471
1309	0.253_2	108.9	323.03	0.9475

Table III.6

Concentration Dependence of D_{12} for Kr-H_2 at 300K

Expt. #	x_1	P	T	D_{12}
1239	0.050_4	108.8	299.98	0.7263
1232	0.100_7	108.6	299.98	0.7275
1233	0.152_5	108.8	299.98	0.7290
1235	0.251_8	108.8	299.98	0.7310
1241	0.401_0	109.0	299.98	0.7350
1242	0.486_9	127.4	299.98	0.7355
1234	0.914_8	106.8	299.98	0.7394
1237	0.949_3	108.5	299.98	0.7400
1238	0.949_8	108.4	299.98	0.7397
1235	0.952_1	108.6	299.98	0.7397

Table III.7

Temperature Dependence of D_{12} for Kr-H_2

Expt. #	x_1	P	T	D_{12}
1387	0.048_9	96.3	278.00	0.6337
1383	0.073_7	96.4	282.86	0.6542
1381	0.074_4	96.4	282.86	0.6551
1379	0.099_5	101.3	286.98	0.6725
1380	0.099_5	101.3	286.98	0.6728
1377	0.101_2	101.5	291.17	0.6898
1378	0.098_5	101.3	291.17	0.6898
1375	0.149_0	101.4	294.96	0.7069
1376	0.148_9	101.4	294.96	0.7072
1373	0.149_6	101.5	302.72	0.7404
1374	0.149_0	101.4	302.72	0.7408
1371	0.149_9	101.5	307.15	0.7593
1372	0.150_0	101.5	307.15	0.7591
1368	0.150_0	101.6	311.11	0.7767
1369	0.150_2	101.6	311.11	0.7768
1366	0.150_7	105.4	314.80	0.7924
1367	0.150_5	105.4	314.80	0.7920
1364	0.150_8	105.4	319.20	0.8120
1362	0.151_0	105.5	323.15	0.8312
1363	0.151_2	105.5	323.15	0.8310

Table III.8

Concentration Dependence of D_{12} for Xe-H_2 at 300K

Expt. #	x_1	P	T	D_{12}
1244	0.050_9	108.4	299.98	0.6248
1253	0.063_1	108.5	299.98	0.6255
1246	0.075_8	108.4	299.98	0.6261
1245	0.101_5	108.6	299.98	0.6273
1242	0.101_6	108.6	299.98	0.6278
1247	0.209_0	108.6	299.98	0.6298
1248	0.403_4	109.0	299.98	0.6338
1248B	0.600_0	163.3	299.98	0.6379
1249	0.950_0	108.4	299.98	0.6410

Table III.9

Temperature Dependence of D_{12} for Xe-H_2

Expt. #	x_1	P	T	D_{12}
1446	0.039_1	83.9	279.52	0.5503
1447	0.039_6	83.9	279.52	0.5505
1448	0.039_8	84.0	283.56	0.5652
1450	0.039_5	84.0	283.56	0.5649
1451	0.039_5	84.0	287.25	0.5783
1452	0.039_6	84.0	287.25	0.5778
1453	0.059_0	83.9	290.72	0.5911
1454	0.059_6	84.0	290.72	0.5918
1455	0.079_6	84.0	295.60	0.6097
1456	0.080_0	84.0	295.60	0.6100
1457	0.079_8	84.0	295.60	0.6098
1427	0.100_1	83.7	304.12	0.6405
1428	0.100_3	83.7	304.12	0.6410
1429	0.124_8	83.7	307.98	0.6568
1430	0.124_8	83.7	307.97	0.6566
1431	0.150_8	83.7	312.00	0.6720
1438	0.151_0	83.8	312.00	0.6720
1440	0.151_5	83.8	316.31	0.6893
1441	0.151_1	83.8	316.31	0.6893

Table III.9 cont.

1442	0.201_2	84.0	319.24	0.7020
1443	0.201_8	84.0	319.24	0.7019
1444	0.226_7	84.2	323.15	0.7191
1445	0.227_2	84.2	323.15	0.7193

Table III.10

Concentration Dependence of D_{12} for Ne-D_2 at 300K

Expt.	x_1	P	T	D_{12}
1483	0.099_6	76.6	300.00	0.8752
1484	0.150_0	76.6	300.00	0.8757
1473	0.150_0	76.6	300.00	0.8767
1474	0.250_6	76.6	300.00	0.8781
1479	0.349_7	76.6	300.00	0.8813
1480	0.449_8	90.5	300.00	0.8840
1482	0.550_9	90.7	300.00	0.8854
1481	0.651_8	76.7	300.00	0.8869
1475	0.751_2	76.5	300.00	0.8884

Table III.11

Concentration Dependence of D_{12} for Ar-D_2 at 300K

Expt. #	x_1	P	T	D_{12}
1471	0.059_8	79.5	300.00	0.5966
1469	0.074_8	79.5	300.00	0.5969
1460	0.099_9	79.5	300.00	0.5978
1458	0.149_9	79.5	300.00	0.5990
1459	0.149_8	79.5	300.00	0.5991
1461	0.249_9	79.5	300.00	0.6018
1466	0.299_8	79.5	300.00	0.6019
1468	0.600_0	119.3	300.00	0.6065
1464	0.850_2	79.5	300.00	0.6073
1462	0.900_4	79.5	300.00	0.6083
1463	0.900_3	79.5	300.00	0.6086

Table III.12

Concentration Dependence of D_{12} for Kr-D_2 at 300K

Expt. #	x_1	P	T	D_{12}
1488	0.099_9	60.5	300.00	0.5195
1486	0.099_9	60.5	300.00	0.5201
1485	0.200_2	60.5	300.00	0.5205
1487	0.300_1	60.5	300.00	0.5215
1492	0.350_4	60.4	300.00	0.5230
1491	0.800_0	60.5	300.00	0.5259
1490	0.800_5	60.5	300.00	0.5262
1489	0.900_4	60.5	300.00	0.5272

Table III.13

Concentration Dependence of D_{12} for Xe-D_2 at 300K

Expt. #	x_1	P	T	D_{12}
1691	0.077_9	210.1	300.00	0.4473
1692	0.078_6	210.0	300.00	0.4477
1521	0.100_3	209.2	300.00	0.4472
1522	0.250_7	209.3	300.00	0.4486
1523	0.250_7	209.3	300.00	0.4490
1524	0.750_1	146.3	300.00	0.4512
1525	0.899_7	209.2	300.00	0.4522
1693	0.953_3	210.4	300.01	0.4515
1695	0.985_2	209.9	300.01	0.4513

Table III.14

Concentration Dependence of D_{12} for Ne-N_2 at 300K

Expt. #	x_1	P	T	D_{12}
1588	0.149_5	176.5	300.01	0.3398
1589	0.149_6	176.5	300.01	0.3398
1587	0.149_8	176.5	300.01	0.3400
1591	0.250_2	176.4	300.01	0.3399
1590	0.749_5	176.4	300.01	0.3399

Table III.15

Temperature Dependence of D_{12} for Ne-N_2

Expt. #	x_1	P	T	D_{12}
1602	0.147_9	176.2	277.10	0.2968
1603	0.099_3	176.3	277.11	0.2968
1604	0.098_9	176.2	277.11	0.2967
1605	0.098_9	176.3	282.92	0.3076
1606	0.099_2	176.3	282.92	0.3079
1607	0.099_3	176.2	282.92	0.3079
1608	0.097_1	176.4	288.97	0.3189
1609	0.099_0	176.4	288.97	0.3190
1611	0.149_8	176.5	295.39	0.3312
1612	0.149_7	176.4	295.39	0.3312
1613	0.200_8	176.7	306.19	0.3520
1614	0.200_8	176.7	306.19	0.3518
1615	0.251_1	176.7	312.04	0.3630
1616	0.297_0	177.4	312.04	0.3631
1617	0.352_2	177.2	312.04	0.3629
1618	0.352_4	177.3	317.18	0.3736
1619	0.350_0	177.3	317.18	0.3733

Table III.16

Concentration Dependence of D_{12} for Kr-N_2 at 300K

Expt. #	x_1	P	T	D_{12}
1512	0.099_3	77.2	300.00	0.1596
1511	0.099_7	77.1	300.00	0.1596
1592	0.100_0	77.1	300.01	0.1595
1594	0.249_9	77.1	300.01	0.1598
1595	0.749_9	77.1	300.01	0.1602
1593	0.899_8	77.2	300.01	0.1603

Table III.17

Temperature Dependence of D_{12} for Kr-N_2

Expt. #	x_1	P	T	D_{12}
1637	0.059_2	77.0	278.73	0.1392
1638	0.059_2	77.0	278.74	0.1394
1632	0.075_9	77.0	283.74	0.1442
1635	0.075_3	77.0	283.74	0.1440
1636	0.074_0	77.0	283.74	0.1439
1630	0.098_8	77.1	289.30	0.1493
1631	0.098_7	77.1	289.30	0.1493
1628	0.150_4	77.1	295.13	0.1549
1629	0.099_5	77.1	295.13	0.1549
1626	0.255_0	77.2	306.10	0.1657
1627	0.200_2	77.2	306.10	0.1657
1624	0.291_2	77.9	312.14	0.1717
1625	0.296_9	77.3	312.14	0.1717
1622	0.296_1	77.7	318.06	0.1778
1623	0.296_3	77.6	318.05	0.1777
1620	0.255_3	77.2	323.08	0.1827
1621	0.302_7	77.5	323.08	0.1828

Table III.18

Concentration Dependence of D_{12} for Xe-N_2 at 300K

Expt. #	x_1	P	T	D_{12}
1599	0.103_1	58.5	300.01	0.1317
1596	0.103_8	58.4	300.01	0.1317
1513	0.150_8	58.4	300.00	0.1320
1600	0.261_9	71.1	300.01	0.1321
1598	0.749_8	69.8	300.01	0.1323
1597	0.896_0	58.4	300.01	0.1325

Table III.19

Temperature Dependence of D_{12} for Xe-N_2

Expt. #	x_1	P	T	D_{12}
1639	0.067_4	59.5	278.50	0.1149
1640	0.039_7	58.4	278.50	0.1149
1641	0.061_1	58.5	284.44	0.1194
1642	0.060_0	58.5	284.44	0.1194
1644	0.059_9	58.5	289.43	0.1232
1645	0.060_6	58.5	289.43	0.1233
1646	0.075_8	58.6	295.24	0.1279
1647	0.041_5	56.7	295.24	0.1276
1648	0.076_4	58.5	295.24	0.1276
1649	0.075_7	58.6	295.24	0.1279
1650	0.099_9	58.5	306.15	0.1368
1651	0.099_9	58.5	306.15	0.1368
1652	0.125_7	58.5	311.89	0.1414
1653	0.128_3	58.7	311.89	0.1416
1654	0.150_7	62.6	317.58	0.1465
1655	0.169_8	62.7	317.58	0.1464
1656	0.200_8	62.7	323.11	0.1512
1657	0.202_9	62.7	323.11	0.1512

APPENDIX IV

Two Bulb Thermal Diffusion Data

The data summarised in section 7.4 are presented in the following tables. The values of x_1 and x_1' for each experiment indicate magnitudesof the separations measured. Second virial coefficient data necessary for calculation of the mole fractions of the calibration mixtures are given in Tables IV.1 and IV.11; literature from which the virial coefficients are taken is cited in these tables.

Although the presentation of α_T to four decimal places is not strictly correct (when compared with $\delta(\alpha_T)$) the precision of the $(\alpha_T)^{-1}$vs x_1 data justifies this.

All symbols in Tables IV.3 to IV.9 are defined here.

x_1 : Mole fraction of the heavy component in the lower (colder) bulb at the end of an experiment.

x_1' : Mole fraction of the heavy component in the upper (hotter) bulb at the end of an experiment.

$\overline{x_1}$: Mean mole fraction for the experiment

$\overline{x_1} = (x_1 + x_1')/2$

$\overline{T}$: Mean temperature to which the experimental α_T value is assigned calculated using equation (3.27).

α_T : The thermal diffusion factor.

$\delta(\alpha_T)$: The error in α_T calculated as outlined in Chapter 6.

t : The time allowed for the attainment of a steady-state (hours).

When calculating (α_T) the error in the mole fractions (see Chapter 6) was generally less than 6×10^{-5}.

Table IV.1

Second Virial Coefficients for Pure Gases used in Equations (5.8) to (5.10)

Gas	$10^4 B_{ii}$ (atm^{-1})	Reference
He	4.67	(1)
Ne	4.59	(1)
Ar	- 6.34	(1)
Kr	-20.5	(1)
Xe	-52.0	(1)
H_2	5.98	(1)
D_2	5.46	(2)
N_2	- 1.70	(1)
CO_2	-49.6	(2)
CH_4	-17.1	(2)

Table IV.2

Interaction Second Virial Coefficients used in Equations (5.8) to (5.10)

System	$10^4 B_{12}'$ (atm^{-1})	Reference
He-Ar	7.38	(3)
Ar-Kr	-11.7	(4)
Ne-H_2	5.82	(4)
Ar-H_2	3.19	(4)
Kr-H_2	1.55	(4)
Xe-H_2	1.01	(4)
Ne-D_2 [a]	5.82	(4)
Ar-D_2	3.19	(4)
Kr-D_2	1.55	(4)
Xe-D_2	1.01	(4)
He-N_2	8.63	(5)
Ne-N_2	5.43	(4)
Ar-N_2	-4.27	(4)
Kr-N_2	-8.95	(4)
Xe-N_2	-13.4	(4)
Ne-CO_2	2.70	(4)

Table IV.2 cont'd.

$He-CH_4$	10.2	(7)
$Ne-CH_4$	6.59	(4)
$Ar-CH_4$	-8.52	(2)
$Kr-CH_4$	-12.6	(4)
$Xe-CH_4$	-20.2	(4)

[a] Experiments show that the interaction virial coefficients for $Ar-D_2$ and $Ar-H_2$ are indistinguishable at 300K[6] and as data for the Rare Gas - D_2 systems are not available in the literature, the corresponding Rare Gas - H_2 values have been used.

Table IV.3

Thermal Diffusion Data for the System He-Ar

Expt. #	x_1	x_1'	$\bar{x}_1$	$\bar{T}$	α_T	$\delta(\alpha_T)$	t
164B	0.19553	0.18329	0.1894	255.3	0.5403	0.007	24.0
164A	0.32590	0.20306	0.2095	255.3	0.5254	0.005	33.0
163B	0.79343	0.78575	0.7896	255.3	0.3136	0.005	23.5
163A	0.81317	0.80611	0.8096	255.3	0.3107	0.005	24.0
145B	0.19753	0.18031	0.1889	270.8	0.5387	0.006	24.0
145A	0.21818	0.20023	0.2029	270.8	0.5200	0.005	32.0
147B	0.49876	0.47814	0.4885	270.8	0.3956	0.004	24.0
147A	0.51879	0.49840	0.5086	270.8	0.3912	0.004	23.0
146B	0.79479	0.78381	0.7893	270.7	0.3160	0.004	29.0
146A	0.81450	0.80442	0.8095	270.8	0.3134	0.004	25.0

Table IV.4

Thermal Diffusion Data for the System Ar-Kr

Expt. #	x_1	x_1'	$\bar{x}_1$	$\bar{T}$	α_T	$\delta(\alpha_T)$	t
166A	0.18579	0.18418	0.1850	255.3	0.0724	0.005	54.5
166B	0.21586	0.21399	0.2149	255.3	0.0751	0.005	96.5
167A	0.78561	0.78404	0.7848	255.3	0.0636	0.006	75.0
167B	0.81563	0.81418	0.8149	255.3	0.0652	0.005	76.0
166E	0.19517	0.19268	0.1939	300.0	0.0945	0.004	71.5
166C	0.20109	0.19841	0.1998	300.0	0.0994	0.004	56.0
167D	0.79566	0.79341	0.7945	300.0	0.0817	0.005	71.0
167E	0.80608	0.80400	0.8050	300.0	0.0786	0.005	56.0

Table IV.5

Thermal Diffusion Data for Rare gas - Hydrogen Systems

$Ne-H_2$

Expt. #	x_1	x_1'	$\bar{x}_1$	$\bar{T}$	α_T	$\delta(\alpha_T)$	t
94A	0.20557	0.19590	0.2007	300.8	0.3408	0.005	24.0
94B	0.20598	0.19626	0.2011	300.8	0.3420	0.005	25.5
95B	0.80681	0.79869	0.8028	300.8	0.2900	0.005	24.0
95A	0.80973	0.80174	0.8057	300.8	0.2886	0.005	22.0

$Ar-H_2$

Expt. #	x_1	x_1'	$\bar{x}_1$	$\bar{T}$	α_T	$\delta(\alpha_T)$	t
83B	0.20486	0.19384	0.1994	300.8	0.3909	0.005	23.5
83A	0.20500	0.29393	0.1995	300.8	0.3926	0.006	29.0
76A	0.50551	0.49197	0.4987	300.8	0.3064	0.004	24.0
89B	0.50577	0.49232	0.4990	300.8	0.3042	0.004	24.0
89A	0.50676	0.49320	0.5000	300.8	0.3066	0.003	23.0
88B	0.80540	0.79827	0.8018	300.8	0.2537	0.004	23.5
88A	0.80637	0.79922	0.8028	300.8	0.2554	0.004	26.0

$Kr-H_2$

Expt. #	x_1	x_1'	$\bar{x}_1$	$\bar{T}$	α_T	$\delta(\alpha_T)$	t
90B	0.19951	0.18829	0.1939	300.8	0.4059	0.005	22.0
90A	0.20289	0.19151	0.1972	300.8	0.4065	0.005	23.0
91A	0.80542	0.79864	0.8020	300.8	0.2414	0.003	27.5
91B	0.80542	0.79865	0.8020	300.8	0.2411	0.003	22.0

$Xe-H_2$

Expt. #	x_1	x_1'	$\bar{x}_1$	$\bar{T}$	α_T	$\delta(\alpha_T)$	t
92A	0.20362	0.19178	0.1977	300.8	0.4220	0.006	23.5
92B	0.20434	0.19251	0.1984	300.8	0.4205	0.006	23.0
93A	0.80227	0.79558	0.7989	300.8	0.2355	0.003	23.0
93B	0.80669	0.80014	0.8034	300.8	0.2345	0.004	22.5

Table IV.6

Thermal Diffusion Data for Rare Gas - Deuterium Systems

$Ne-D_2$

Expt. #	x_1	x_1'	$\bar{x}_1$	$\bar{T}$	α_T	$\delta(\alpha_T)$	t
120B	0.19305	0.18524	0.1892	300.9	0.2864	0.005	23.5
120C	0.20298	0.19843	0.1989	300.9	0.2877	0.005	24.0
121B	0.79276	0.78531	0.7890	300.0	0.2518	0.005	24.0
121A	0.81263	0.80574	0.8092	300.9	0.2511	0.005	24.0

$Ar-D_2$

Expt. #	x_1	x_1'	$\bar{x}_1$	$\bar{T}$	α_T	$\delta(\alpha_T)$	t
119B	0.19403	0.18246	0.1891	300.9	0.3583	0.005	23.0
119A	0.21437	0.20386	0.2091	300.9	0.3575	0.005	31.0
118B	0.79281	0.78574	0.7893	300.9	0.2391	0.004	24.0
118A	0.81270	0.80620	0.8095	300.9	0.2371	0.004	24.5

$Kr-D_2$

Expt. #	x_1	x_1'	$\bar{x}_1$	$\bar{T}$	α_T	$\delta(\alpha_T)$	t
124A	0.19469	0.18405	0.1894	300.9	0.3899	0.005	47.5
124B	0.21477	0.20349	0.2091	300.9	0.3838	0.005	54.5
126A	0.79313	0.78614	0.7896	300.9	0.2367	0.004	48.0
126B	0.81287	0.80643	0.8097	300.9	0.2350	0.004	48.0

$Xe-D_2$

Expt. #	x_1	x_1'	$\bar{x}_1$	$\bar{T}$	α_T	$\delta(\alpha_T)$	t
122A	0.19490	0.18358	0.1892	300.9	0.4151	0.005	33.5
122B	0.21513	0.20318	0.2092	300.9	0.4065	0.005	48.5
123A	0.79312	0.78626	0.7897	300.9	0.2324	0.004	49.5
123B	0.81279	0.80651	0.8097	300.9	0.2292	0.004	48.0

Table IV.7

Thermal Diffusion Data for Rare Gas - Nitrogen Systems

$He-N_2$

Expt. #	x_1	x_1'	$\bar{x}_1$	$\bar{T}$	α_T	$\delta(\alpha_T)$	t
154B	0.19498	0.18271	0.1888	254.2	0.5116	0.007	24.5
154C	0.20561	0.19260	0.1991	253.5	0.5023	0.006	24.5
154A	0.21569	0.20300	0.2093	254.1	0.4882	0.006	25.0
155B	0.79351	0.78565	0.7896	253.7	0.2948	0.005	23.5
155A	0.81322	0.80618	0.8097	254.0	0.2883	0.005	26.5
96A	0.20501	0.19088	0.1979	300.8	0.5033	0.006	23.5
96B	0.20728	0.19305	0.2002	300.8	0.5027	0.006	25.5
67B	0.50686	0.49050	0.4987	300.8	0.3701	0.003	24.5
65B	0.80302	0.79467	0.7988	300.8	0.2939	0.005	24.5
65C	0.80301	0.79467	0.7988	300.8	0.2935	0.005	23.5
65A	0.80323	0.79480	0.7991	300.8	0.2938	0.005	23.5
97B	0.80653	0.79834	0.8024	300.8	0.2921	0.004	25.0

$Ne-N_2$

Expt. #	x_1	x_1'	$\bar{x}_1$	$\bar{T}$	α_T	$\delta(\alpha_T)$	t
160B	0.18566	0.18405	0.1849	255.3	0.0724	0.005	30.0
160C	0.20079	0.19914	0.2000	255.3	0.0699	0.004	24.0
160A	0.21583	0.21406	0.2149	255.3	0.0710	0.005	46.5
159B	0.78537	0.78406	0.7847	255.3	0.0525	0.004	24.0
159C	0.80059	0.79931	0.8000	255.3	0.0542	0.004	50.0
159A	0.81550	0.81433	0.8149	255.3	0.0526	0.005	31.5
150B	0.18608	0.18368	0.1849	270.8	0.0764	0.005	24.0
150A	0.21600	0.21336	0.2147	270.8	0.0750	0.004	24.5
151B	0.78582	0.78389	0.7849	270.8	0.0548	0.003	25.0
151A	0.81574	0.81402	0.8149	270.8	0.0546	0.004	24.0
107A	0.20099	0.19872	0.1999	300.9	0.0798	0.005	23.5
107B	0.20108	0.19883	0.2000	300.9	0.0791	0.005	23.0
117B	0.48620	0.48318	0.4847	300.9	0.0680	0.004	29.0
117A	0.51623	0.51324	0.5147	300.9	0.0673	0.004	48.0
108A	0.80065	0.79899	0.7998	300.9	0.0583	0.004	24.0
108B	0.80059	0.79892	0.7998	300.9	0.0586	0.004	32.0

$Ar-N_2$

Expt. #	x_1	x_1'	$\bar{x}_1$	$\bar{T}$	α_T	$\delta(\alpha_T)$	t
161B	0.18073	0.17929	0.1800	255.3	0.0662	0.005	49.5
161A	0.22069	0.21901	0.2199	255.3	0.0664	0.006	47.5
165B	0.78074	0.77896	0.7799	255.3	0.0703	0.005	75.0
165A	0.82060	0.81905	0.8198	255.3	0.0711	0.007	48.5
168B	0.18097	0.17887	0.1799	270.8	0.0682	0.004	51.0
168A	0.22116	0.21863	0.2199	270.8	0.0707	0.004	55.0
149B	0.78119	0.77858	0.7799	270.8	0.0728	0.004	72.0
149A	0.82079	0.81878	0.8199	279.8	0.0711	0.004	49.5
106B	0.20078	0.19865	0.1997	300.9	0.0750	0.007	24.0
106A	0.20089	0.19875	0.1998	300.9	0.0753	0.005	23.0
104A	0.50144	0.49804	0.4997	300.9	0.0765	0.004	30.0
104B	0.50146	0.49809	0.4998	300.9	0.0758	0.004	24.0
105B	0.80092	0.79871	0.7998	300.9	0.0776	0.005	30.0
105A	0.80095	0.79873	0.7998	300.9	0.0780	0.005	29.0

$Kr-N_2$

Expt. #	x_1	x_1'	$\bar{x}_1$	$\bar{T}$	α_T	$\delta(\alpha_T)$	t
152D	0.18951	0.18661	0.1881	254.1	0.1207	0.004	72.0
152C	0.20127	0.19828	0.1998	254.3	0.1198	0.005	48.0
153D	0.79545	0.79258	0.7940	254.1	0.1115	0.004	74.0
152A	0.18674	0.18269	0.1847	270.8	0.1289	0.004	47.5
152B	0.21701	0.21248	0.2147	270.8	0.1287	0.003	48.5
153A	0.78680	0.78272	0.7848	270.8	0.1158	0.003	48.0
153B	0.81656	0.81299	0.8148	270.8	0.1134	0.004	48.0
114A	0.18672	0.18276	0.1847	300.9	0.1479	0.004	71.0
114C	0.20204	0.19786	0.2000	300.9	0.1470	0.005	82.0
113B	0.48765	0.48155	0.4846	300.9	0.1373	0.003	71.0
113A	0.50254	0.49645	0.4995	300.9	0.1370	0.003	72.5
113C	0.51757	0.51145	0.5145	300.9	0.1378	0.003	73.0
115A	0.78667	0.78273	0.7847	300.9	0.1312	0.004	71.0
115B	0.81653	0.81300	0.8148	300.9	0.1316	0.005	72.0

Xe-N_2

Expt. #	x_1	x_1'	$\bar{x}_1$	$\bar{T}$	α_T	$\delta(\alpha_T)$	t
156A	0.18651	0.18317	0.1848	253.2	0.1344	0.004	47.5
156B	0.21672	0.21303	0.2149	253.6	0.1352	0.004	73.5
157A	0.78625	0.78310	0.7847	253.2	0.1132	0.005	71.5
157B	0.81608	0.81342	0.8148	253.2	0.1071	0.005	54.0
156C	0.20199	0.19757	0.1998	274.2	0.1526	0.004	68.5
156D	0.20279	0.19834	0.2006	274.2	0.1531	0.004	71.5
157D	0.79715	0.79357	0.7954	274.2	0.1214	0.004	70.0
157C	0.80147	0.79792	0.7997	274.3	0.1224	0.004	73.0
111E	0.18695	0.18829	0.1846	300.9	0.1742	0.005	95.5
111D	0.20219	0.19724	0.1997	300.9	0.1742	0.004	73.5
112A	0.78670	0.78257	0.7846	300.9	0.1375	0.004	74.0
112C	0.80160	0.79771	0.7997	300.9	0.1366	0.005	50.0
112B	0.81646	0.81281	0.8146	300.9	0.1359	0.005	72.0

Table IV.8

Thermal Diffusion Data for the System Ne-CO_2

Expt. #	x_1	x_1'	$\bar{x}_1$	$\bar{T}$	α_T	$\delta(\alpha_T)$	t
144A	0.19269	0.18659	0.1896	270.8	0.1903	0.004	48.0
144B	0.20261	0.19620	0.1994	270.8	0.1924	0.004	48.0
143A	0.79746	0.79325	0.7954	270.8	0.1239	0.003	75.0
143B	0.80718	0.80317	0.8052	270.8	0.1226	0.003	46.5
140B	0.19249	0.18696	0.1897	300.9	0.2023	0.004	46.0
140A	0.21265	0.20679	0.2097	300.9	0.1989	0.004	49.0
139B	0.79733	0.79359	0.7955	300.9	0.1293	0.003	48.5
139A	0.81671	0.81330	0.8150	300.9	0.1272	0.004	45.5
141A	0.20220	0.19712	0.1997	324.4	0.2054	0.005	50.5
141B	0.21217	0.20695	0.2096	324.4	0.2045	0.004	48.0
142A	0.80692	0.80373	0.8053	324.3	0.1322	0.005	48.0
142B	0.81659	0.81353	0.8151	324.3	0.1318	0.005	46.0

Table IV.9

Thermal Diffusion Data for Rare Gas - Methane Systems

$He-CH_4$

Expt. #	x_1	x_1'	$\bar{x}_1$	$\bar{T}$	α_T	$\delta(\alpha_T)$	t
130A	0.19127	0.17977	0.1855	300.9	0.4282	0.005	23.0
130B	0.21976	0.20727	0.2135	300.9	0.4183	0.005	26.0
129A	0.79015	0.78274	0.7864	300.9	0.2482	0.004	27.5
129B	0.81952	0.81304	0.8163	300.9	0.2430	0.005	24.0

$Ne-CH_4$

Expt. #	x_1	x_1'	$\bar{x}_1$	$\bar{T}$	α_T	$\delta(\alpha_T)$	t
133A	0.17032	0.16978	0.1701	300.9	0.0215	0.007	24.0
133B	0.23044	0.22973	0.2301	300.9	0.0225	0.005	29.0
134C	0.80043	0.79943	0.7999	300.9	0.0352	0.004	27.5
134B	0.83032	0.82943	0.8229	300.9	0.0354	0.004	22.0

$Ar-CH_4$

Expt. #	x_1	x_1'	$\bar{x}_1$	$\bar{T}$	α_T	$\delta(\alpha_T)$	t
103B	0.18635	0.18349	0.1849	300.9	0.1068	0.005	47.5
103C	0.21640	0.21325	0.2148	300.9	0.1051	0.004	48.5
128B	0.48701	0.48232	0.4847	300.9	0.1056	0.003	47.0
128A	0.51712	0.51286	0.5148	300.9	0.1049	0.003	48.5
127B	0.78631	0.78311	0.7847	300.9	0.1065	0.004	48.0
127A	0.81614	0.81329	0.8147	300.9	0.1062	0.005	47.0

$Kr-CH_4$

Expt. #	x_1	x_1'	$\bar{x}_1$	$\bar{T}$	α_T	$\delta(\alpha_T)$	t
131A	0.18499	0.18159	0.1833	300.9	0.1277	0.004	69.0
131B	0.21492	0.21112	0.2130	300.9	0.1275	0.004	77.0
132A	0.78900	0.78575	0.7874	300.9	0.1092	0.004	71.0
132B	0.80902	0.80603	0.8075	300.9	0.1082	0.004	72.0

Xe-CH_4

Expt. #	x_1	x_1'	$\bar{x}_1$	$\bar{T}$	α_T	$\delta(\alpha_T)$	t
137A	0.18505	0.18182	0.1834	300.9	0.1212	0.004	76.0
137B	0.21505	0.21150	0.2133	300.9	0.1190	0.003	70.0
138A	0.79115	0.78842	0.7898	300.9	0.0925	0.004	71.0
138B	0.81110	0.80859	0.8098	300.9	0.0916	0.004	81.0

REFERENCES

1. J.H. Dymond and E.B. Smith, *The Virial Coefficients of Gases*, Clarendon Press, Oxford (1969).
2. J.H. Dymondand E.B. Smith, *The Virial Coefficients of Pure Gases and Mixtures*, Oxford University Press, Oxford (1980).
3. J. Brewer and G.W. Vaughn, *J.Chem.Phys.* 50 2960 (1969).
4. J. Brewer, *Determination of Mixed Virial Coefficients*, Report No. MRL-2915-C, Air Force Office of Scientific Research, No. 67-2795 (1967).
5. G.M. Kramer and J.G. Miller, *J.Phys.Chem.* 61 785 (1957).
6. P.J. Dunlop, *unpublished data.*
7. M.L. Martin, R.D. Trengove, K.R. Harris and P.J. Dunlop, *Aust.J.Chem.* 35 1525 (1982).

APPENDIX V

Potential Parameters for Like and Unlike Interactions.

All potential functions used for calculation of transport properties in Chapter 7 are listed in Tables V.1 (like interactions) and V.2 (unlike interactions).

ε/k is the depth of the potential well (K) and

σ is the distance at which the interaction energy is zero (Å)

The references in the tables are the references for the potentials in Chapter 7.

Table V.1[a,b,c]

Potentials for like interactions

	Potential	ε/k	σ	Reference
He	HFD	10.8	2.639	(15)
Ne	HFD	43.0	2.746	(16)
Ar	HFD	143.2$_2$	3.356	(17)
Kr	Barker-K2	201.9	3.573	(18)
Xe	Barker-X2	281.0	3.890	(18)
H_2[a]	exp-6	37.3	2.967	(19)
D_2[b]	exp-6	37.3	2.967	
N_2	(12,6,8,γ=1.5)	116.0	3.561	(20)
CO_2[c]	(m68)	217.0	3.775	(21)
CH_4	(20,6,8,γ=0)	217.0	3.559	(22)

a The quantum collision integrals of Taylor were used for Hydrogen.

b The hydrogen potential is used for deuterium.

c Asymmetric potential; the collision integrals in the literature were used.

Table V.2[a]

Potentials for unlike interactions.

	Potential	ε/k	σ_{12}	Reference
He-Ar	HFD	29.8	3.104	(19)
Ar-Kr	HFD	167.3	3.468	(20)
	MSMV	167.5	3.476	(22)
	MSMSV	167.1	3.460	(23)
	MS	165.0	3.489	(24)
Ne-H_2	LJ(12,6)	43.0	2.85	(35)
	LJ(15,6)	37.3	2.973	(36)
	HFD	33.0_7	2.920	(37)
	(10,6,8,γ=2.0)	34.0	2.858	this study
Ar-H_2	LJ(12,6)	80.0	3.18	(38)
	BC	73.1_5	3.178	(39)
	(12,6,8,γ=2.5)	97.0	2.986	this study
Kr-H_2	LJ(12,6)	87.3	3.30	(40)
	LJ(12,6,8)	83.4_4	3.348	(41)
	BC	84.5_6	3.301	(39)
	(11,6,8,γ=3.0)	101.0	3.159	this study
Xe-H_2	LJ(13,6)	96.5	3.511	(40)
	LJ(12,6,8)	94.0	3.528	(41)
	BC	94.2	3.520	(39)
	HFD	92.4_9	3.59	(38)
	(11,6,8,γ=3.0)	106.0	3.376	this study
He-N_2	SPFD	26.3	3.22	(53)
	11,6,8,γ=0.0	21.0	3.262	(6)
Ne-N_2	12,6,8,γ=0.5	55.0	3.164	this study
Ar-N_2	LJ(12,6)	136.2	3.90	(54)
	LJ(20,6)	138.3	3.90	(54)
	9,6,8,γ=4.0	99.5	3.546	(6)
Kr-N_2	LJ(12,6)	158.6	4.05	(54)
	LJ(20,6)	155.7	4.05	(54)
	15,6,8,γ=0.8	176.0	3.414	this study
Xe-N_2	15,6,8,γ=0.8	190.0	3.622	this study
Ne-CO_2	12,6,8,γ=0.8	63.0	3.345	(60)

	Potential	ε/k	σ_{12}	Reference
He-CH_4	10,6,8,γ=2.0	21.5	3.402	(8)
	LJ(12,6)	31.3	2.985	(61)
	SPFD	23.2	3.40	(60)
Ne-CH_4	20,6,8,γ=0	75.0	3.121	(8)
Ar-CH_4	20,6,8,γ=0	190.0	3.334	(8)
	MSMSV	170.6	3.489	(62)
	MSV	158.7	3.444	(63)
	LJ(12,6)	138.0	4.035	(64)
	LJ(18,6)	164.0	3.513	(65)
Kr-CH_4	11,6,8,γ=0.25	162.0	3.655	(8)
Xe-CH_4	13,6,8,γ=2.0	270.0	3.610	(8)

[a] The potentials listed for the rare gas - hydrogen systems are also used for calculations involving rare gas - deuterium systems.

APPENDIX VI

Source and Purity of Gases used.

Gas	Source	Minimum Purity (as stated by the manufacturer)
He	CIG[a]	99.999%
Ne	Matheson[b]	99.999%
Ar	CIG	99.999%
Kr	Matheson	99.995%
Xe	Matheson	99.9%
H_2	CIG	99.98%
D_2	Matheson	99.5%
N_2	CIG	99.99%
CO_2	CIG	99.8%
CH_4	Matheson	99.99%

[a] The Commonwealth Industrial Gases Limited.

[b] Matheson Division of Searle Medical Products, U.S.A. Inc.